



Summary of Emerging Research Results:

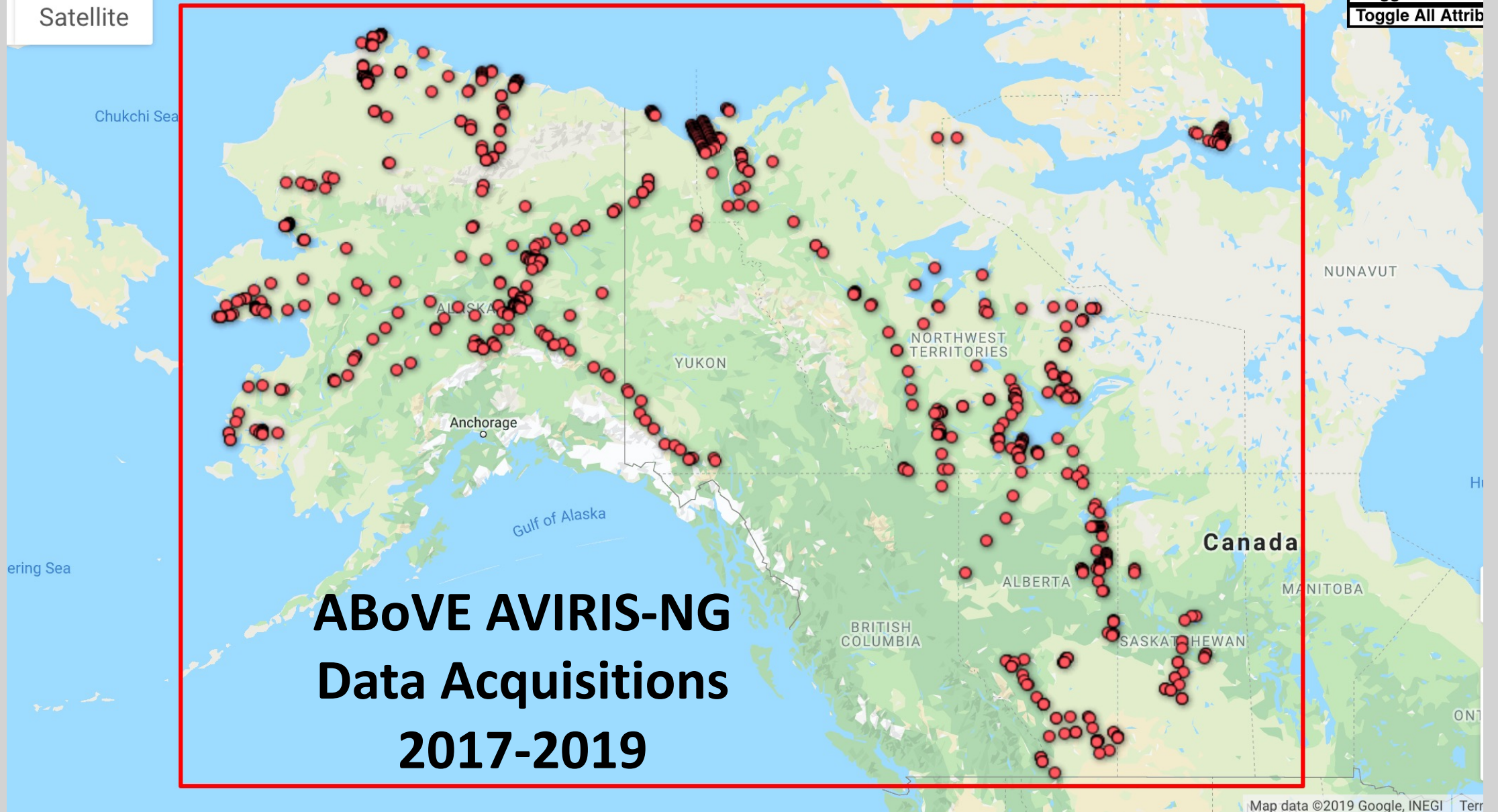
AVIRIS-NG Campaigns over Vegetation 2017-2022

Phil Townsend, Chip Miller and Contributors



Satellite

Toggle All AVIR
Toggle All Attrib

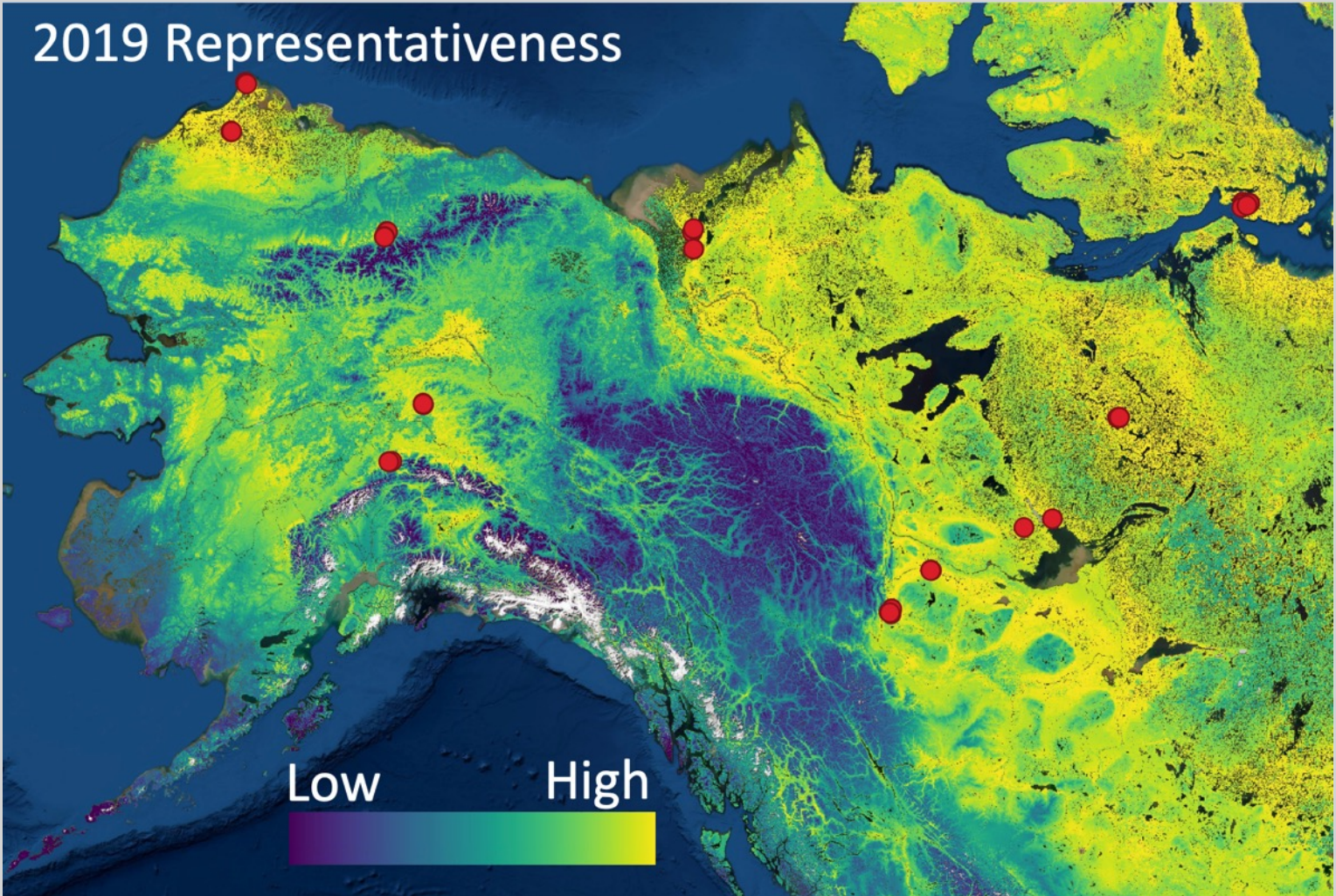


New for 2022:

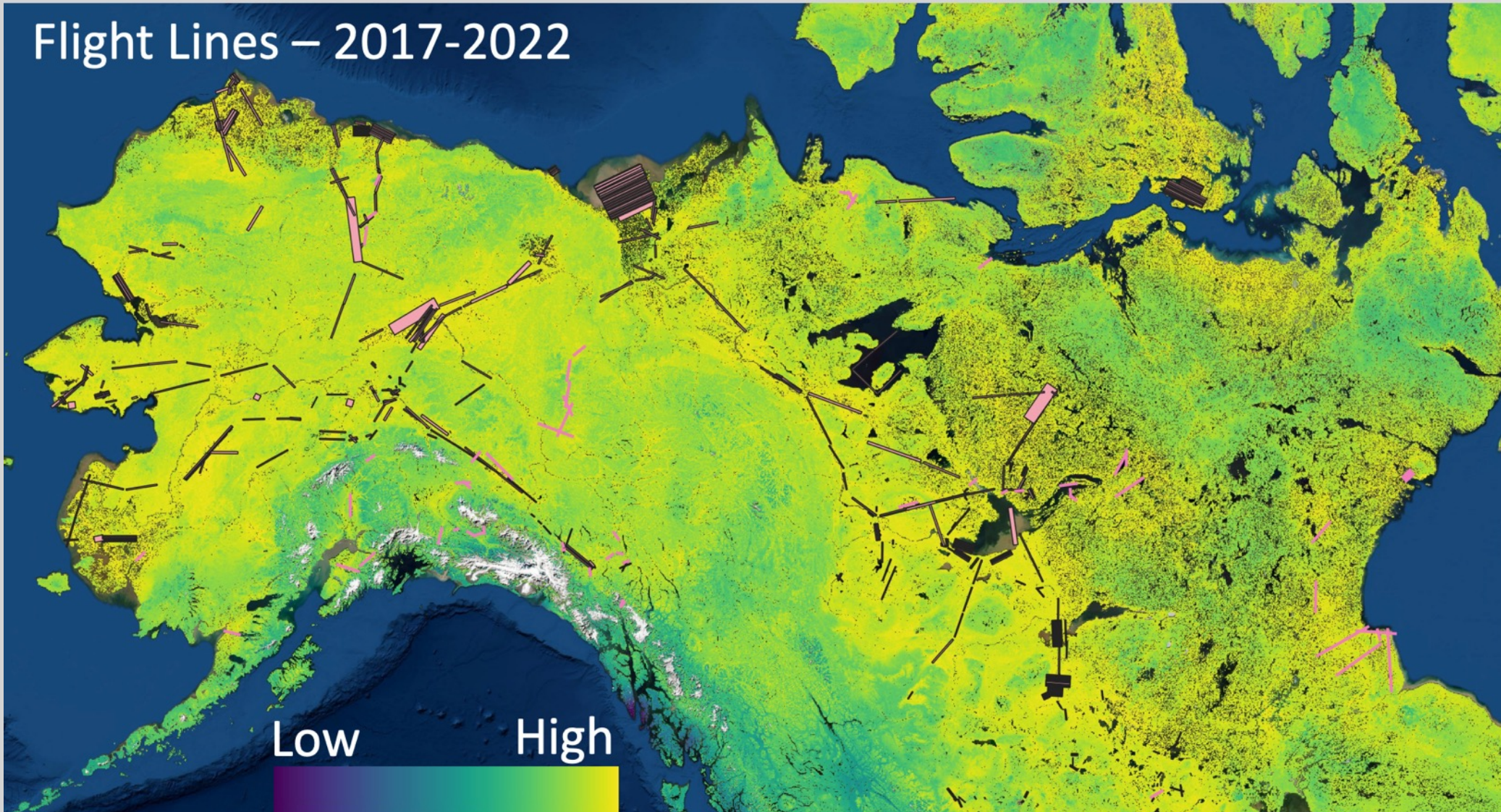
AVIRIS Trait Strategy Fills Representativeness Gaps

Ryan Pavlick (JPL), Kyle Kovach and Phil Townsend (Wisconsin)





Flight Lines – 2017-2022





Four General Areas of Emerging Research

- Image Processing (atmospheric and other corrections)
 - Thompson, Brodrick (JPL), Queally (Wisconsin)
- Species composition and composition change, *and...*
- Upscaling and mapping foliar functional traits
 - Smith, Badola & Panda (UAF); Nelson (Schoodic Institute); Huemmrich, Campbell, Tweedie, Vargas (GSFC/UTEP), Yang & Serbin (BNL); Wenqu Chen and Jennifer Fraterrigo (Illinois); Kyle Kovach, Phil Townsend (Wisconsin) & Ryan Pavlick (JPL)
- Linkage to fluxes (GPP, methane)
 - Miller, Latha Baskaran, Clayton Elder (JPL); Orcutt (Sacramento State), Magney (UC Davis), Frankenburg (CalTech), Maguire (CSP), Pierrat (UCLA)
- Major theme: Scaling: Leaf → Plot → Drone → Airplane → Satellite



Airborne Image Processing

- Challenges of atmospheric corrections in heterogeneous environments (surface and atmosphere)

JGR Biogeosciences

Research Article |  Open Access |   

Atmospheric Lengthscales for Global VSWIR Imaging Spectroscopy

David R. Thompson , Niklas Bohn, Philip G. Brodrick, Nimrod Carmon, Michael L. Eastwood, Regina Eckert, Cédric G. Fichot, Joshua P. Harringmeyer, Hai M. Nguyen, Marc Simard, Andrew K. Thorpe

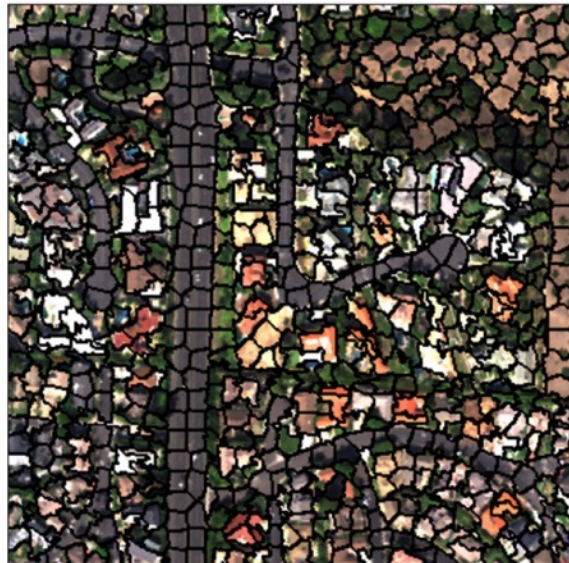
First published: 09 June 2022 | <https://doi.org/10.1029/2021JG006711> | Citations: 1

- Estimation of surface reflectance and atmospheric state is computationally challenging
- ISOFIT uses emulation to capture RTM behavior
- Segmentation is used to preclude inverting every pixel

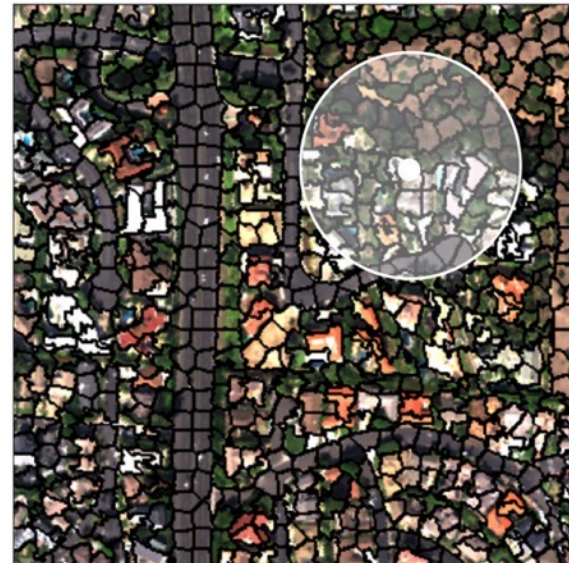
A. Original Image



B. Segmentation



D. Build Local Linear Models



E. Pixelwise Linear Inversion





BRDF, Topographic, Solar Zenith Angle Correction

- ABoVE-wide algorithms require consistent processing across many overlapping flightlines with highly variable surface characteristics

JGR Biogeosciences

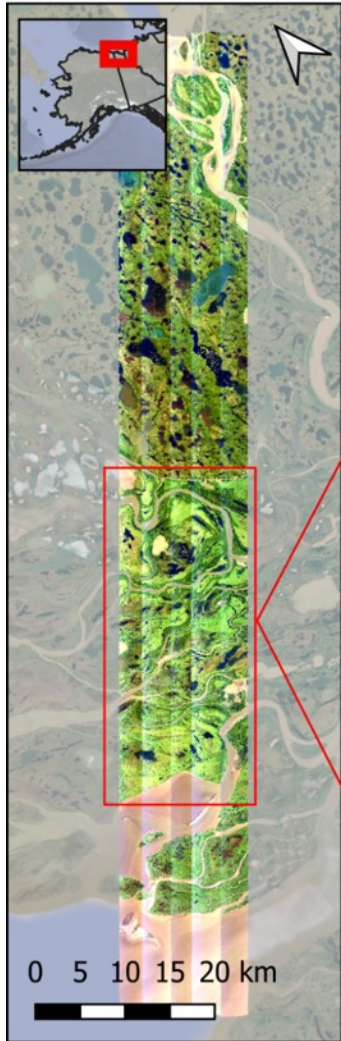
Research Article |  Open Access |  

FlexBRDF: A Flexible BRDF Correction for Grouped Processing of Airborne Imaging Spectroscopy Flightlines

Natalie Queally , Zhiwei Ye, Ting Zheng, Adam Chlus, Fabian Schneider, Ryan P. Pavlick, Philip A. Townsend

First published: 05 January 2022 | <https://doi.org/10.1029/2021JG006622> | Citations: 1

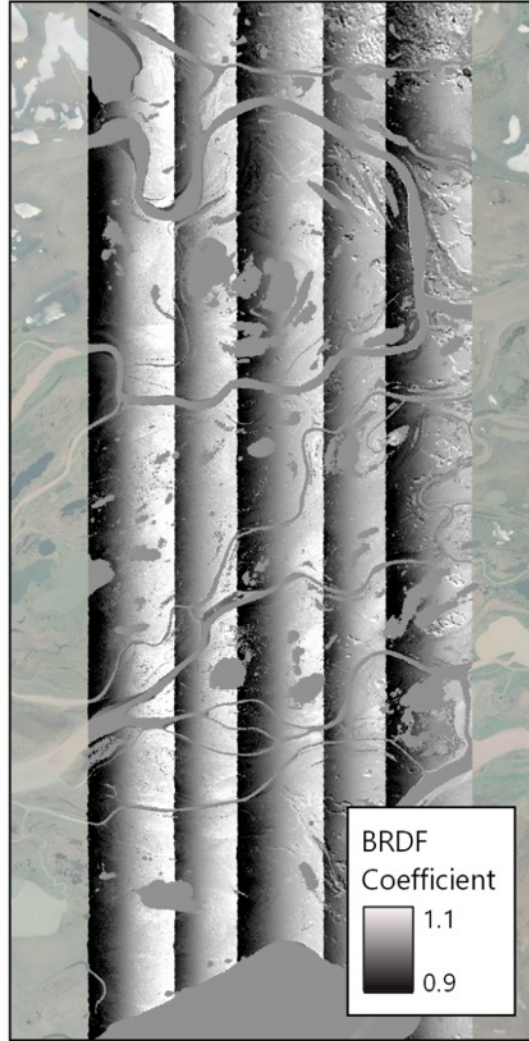
Mackenzie Delta – 26 July 2019



Uncorrected Reflectance



11:17 10:58 10:38 10:19 09:59



Corrected Reflectance





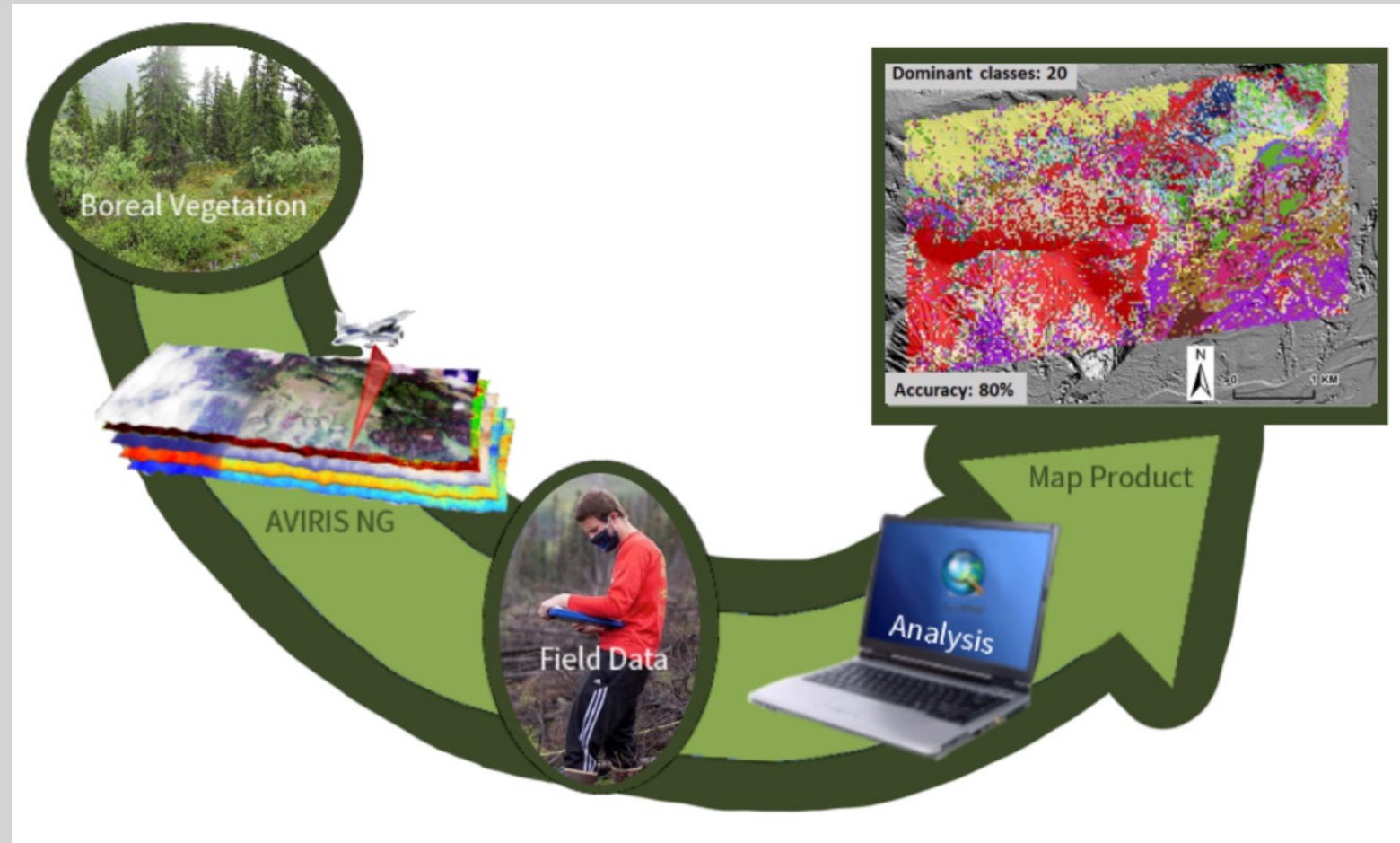
Wildfire Fuel Type

- Santosh Panda, Christopher Smith, Anushree Badola, Uma Bhatt + collaborators (UAF)

- Badola, A., Panda, S.K., Roberts, D.A., Waigl, C., Jandt, R.R., Bhatt, U.S. 2022. A novel method to simulate AVIRIS-NG hyperspectral image from Sentinel-2 image for improved vegetation/wildfire fuel mapping, boreal Alaska. *International Journal of Applied Earth Observation and Geoinformation*,. V. 112 (102891). <https://doi.org/10.1016/j.jag.2022.102891>
- Badola, A., Panda, S.K., Roberts, D.A., Waigl, C., Bhatt, U.S., Smith, C.W., Jandt, R.R. 2021. Hyperspectral data simulation (Sentinel-2 to AVIRIS-NG) for improved wildfire fuel mapping, boreal Alaska. *Remote Sensing*, 13(9): 1693. <https://doi.org/10.3390/rs13091693>
- Smith, C.W., Panda, S.K., Bhatt, U.S., Meyer, F.J. 2021. Improved boreal forest wildfire fuel type mapping using AVIRIS-NG hyperspectral data, interior Alaska. *Remote Sensing*, 13(5): 897. <https://doi.org/10.3390/rs13050897>

Improved Wildfire Fuel Type Mapping using NASA AVIRIS-NG Hyperspectral data, Interior Alaska (Christopher Smith)

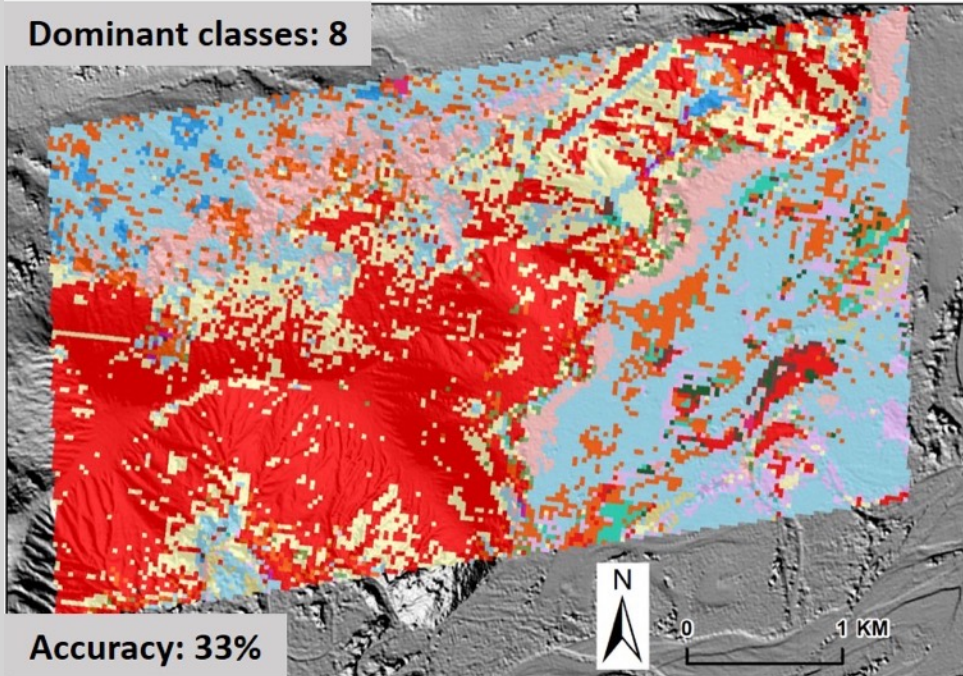
- Urgent need to improve on 30 m Landsat products
- Use RF with AVIRIS-NG to develop vegetation type and fire fuel maps



Comparison of vegetation map products for 2014 LF EVT and AVIRIS-NG 304 band image. Colors represent distinct vegetation classes.

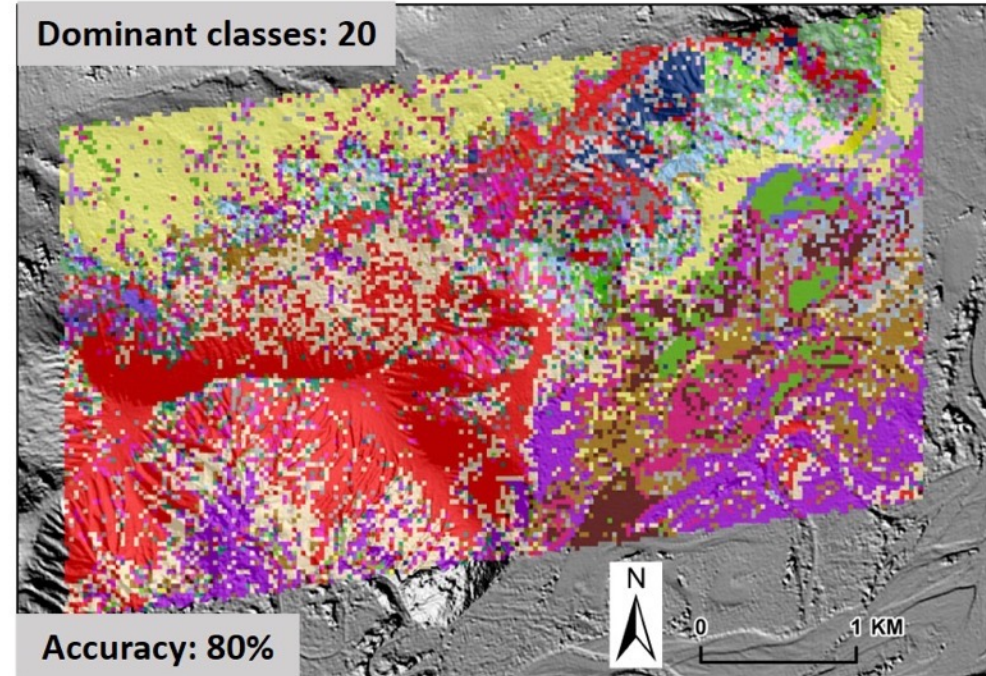
LANDFIRE Existing Vegetation Type (EVT)

Dominant classes: 8



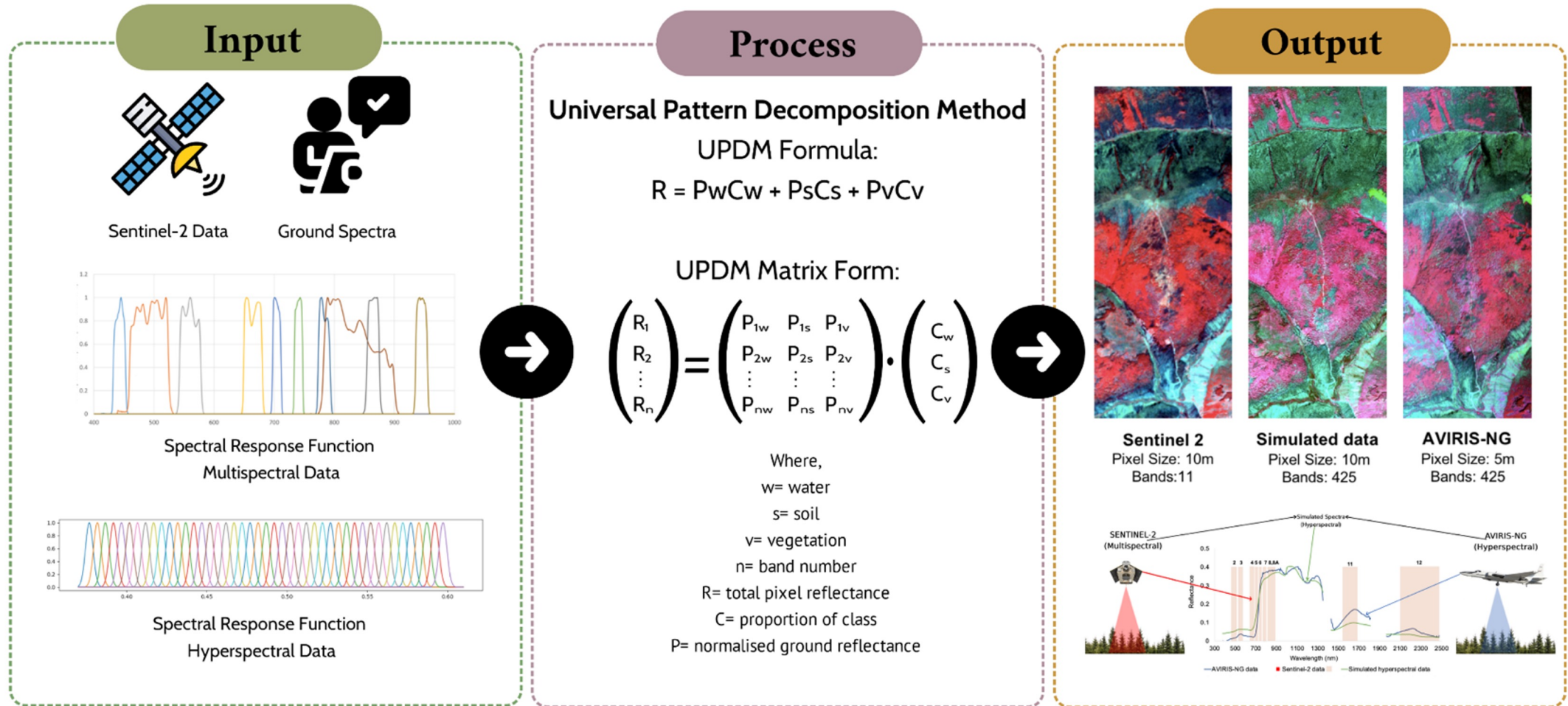
Vegetation classes from AVIRIS-NG 304 Image

Dominant classes: 20



Upscaling improved Vegetation/Fuel Maps for the Boreal Region of Alaska

Research question: How to generate improved vegetation/fuel map for boreal region of Alaska?



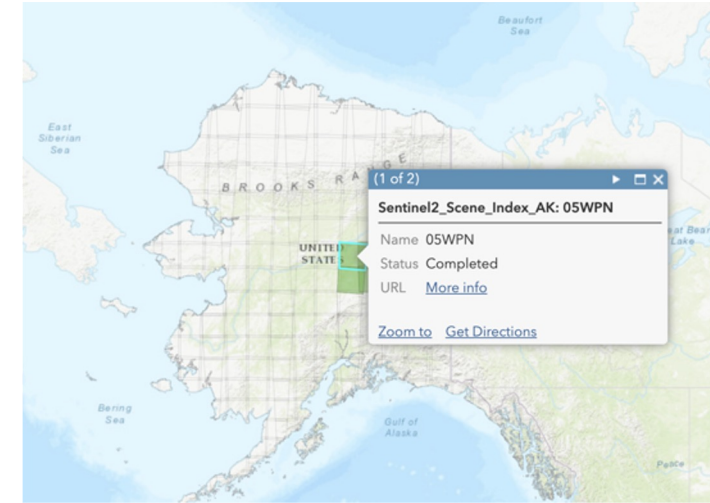
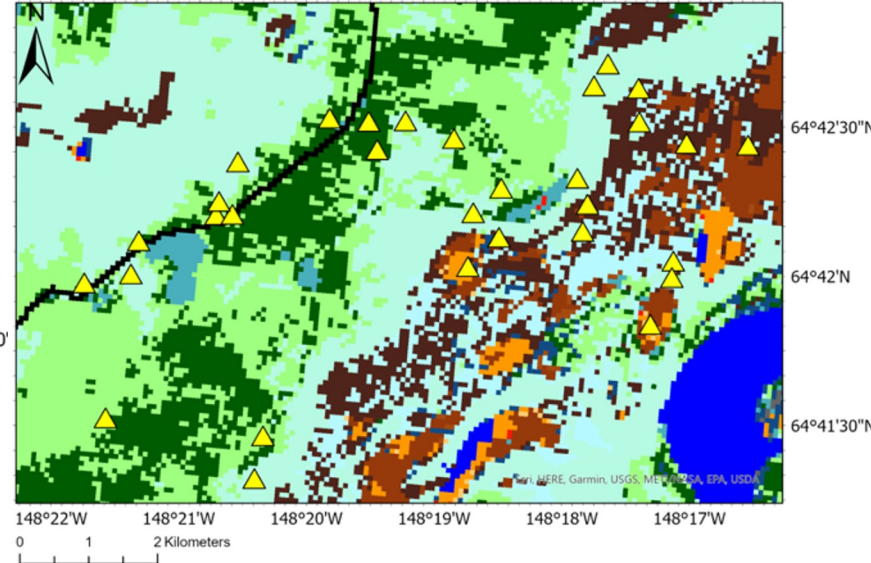
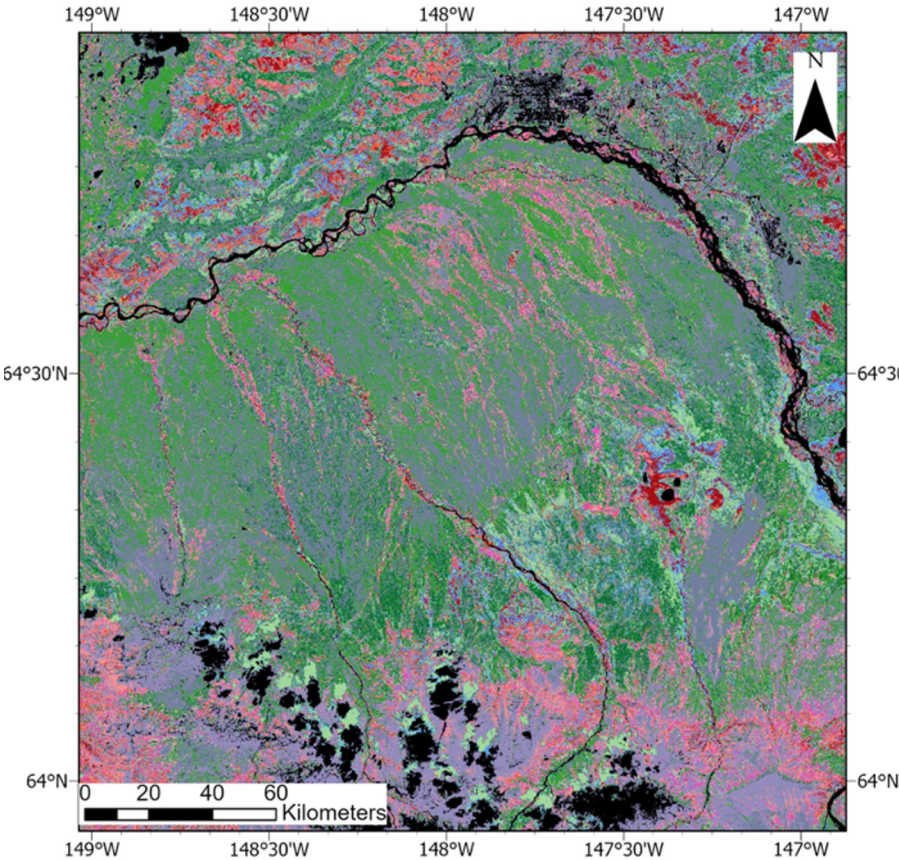
Sentinel-2 to AVIRIS-NG: 2 hours

Badola *et al.*, 2021, Remote Sensing,
<https://doi.org/10.3390/rs13091693>

Vegetation Map, Interior AK

Product Accuracy

Product Sharing



- LANDFIRE EVT Product: **32%** (10 out of 31 plots mapped correctly)
- Classified simulated hyperspectral data: **65%** (20 out of 31 plots mapped correctly)

ArcGIS online
Axiom

Vegetation Classes	
■ Masked	■ Open balsam poplar forest
■ Open black spruce forest	■ Closed paper birch-quaking aspen forest
■ Black spruce woodland	■ Open spruce - balsam poplar forest
■ Closed black spruce forest	■ Open paper birch - quaking aspen forest
■ Closed white spruce forest	■ Open spruce - paper birch forest
■ White spruce woodland	■ Closed spruce - paper birch - quaking aspen forest
■ Open paper birch forest	■ Closed tall alder
■ Open quaking aspen forest	■ Other
	■ Wetlands

A novel pathway to generate low-cost and detailed vegetation/fuel maps for boreal Alaska to aid forest and fire management.



Plant Functional Types and Traits

- High-latitudes regions are warming faster than the rest of the planet, increasing plant trait variation across local to regional scales.
- Plant traits (e.g. leaf nitrogen, leaf phosphorus, specific leaf area) are critical to gross primary production and foliar respiration.
- But knowledge of the distribution of plant traits across rapidly changing tundra ecosystems are limited, yet are essential for improving the performance of carbon cycle processes in Earth System Models.



Plant Functional Types and Traits

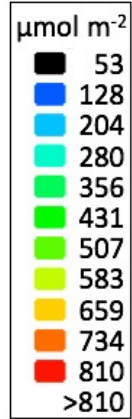
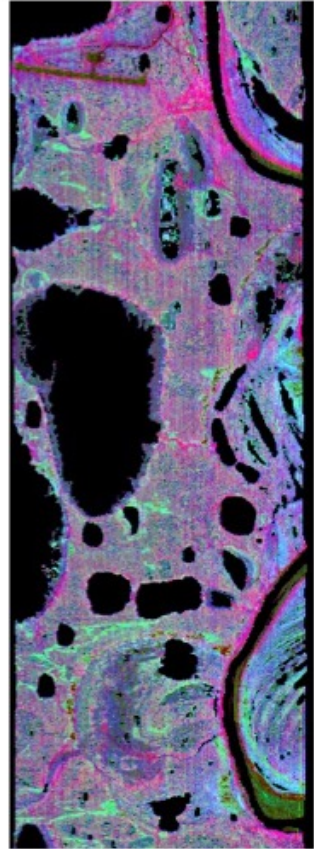
- Fred Huemrich, Petya Campbell, Craig Tweedie, Sergio Vargas + collaborators

Utilizing Spectral Imagery to Examine High Latitude Ecosystem Function and Diversity

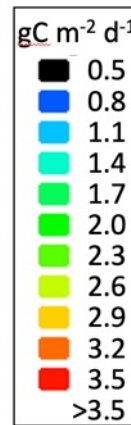
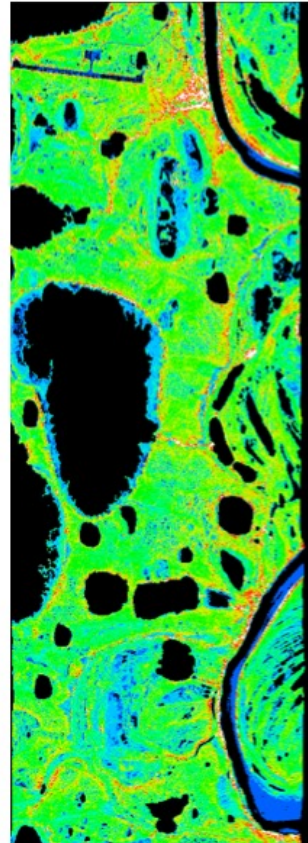
K. F. Huemmrich¹, P. K. E. Campbell¹, S. A. Vargas Z.², C. E. Tweedie², E.M. Middleton³

¹UMBC/Biospheric Sciences Lab NASA GSFC, ²UTEP, ³Biospheric Sciences Lab NASA GSFC

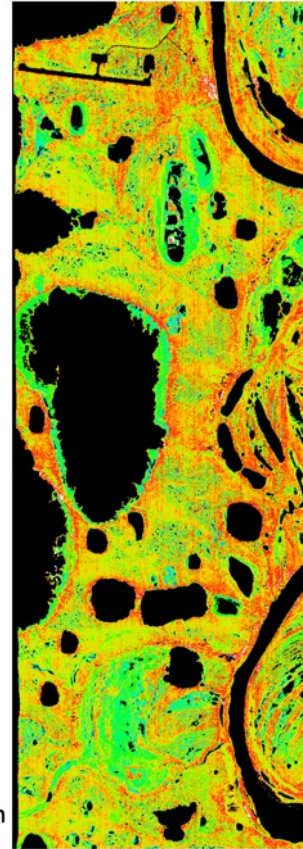
Cover RGB (R=Vascular Plants, G=Lichen)



Chl Content



GPP

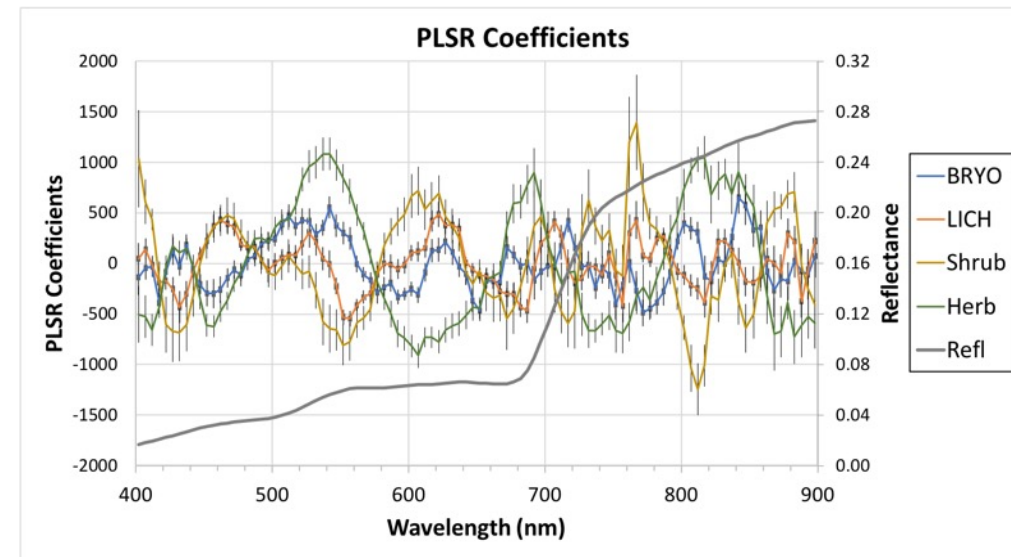


Vegetation percent cover (PLSR): bryophytes, lichens, shrubs, herbs.
RMSE = 22.8%; $R^2 = 0.61$

Chlorophyll content from leaf level Chl measurements (Unispec).
RMSE = 0.59; $R^2 = 137$

GPP from ITEX diurnal plot measurements (IRGA). RMSE = 0.45, $R^2 = 0.70$

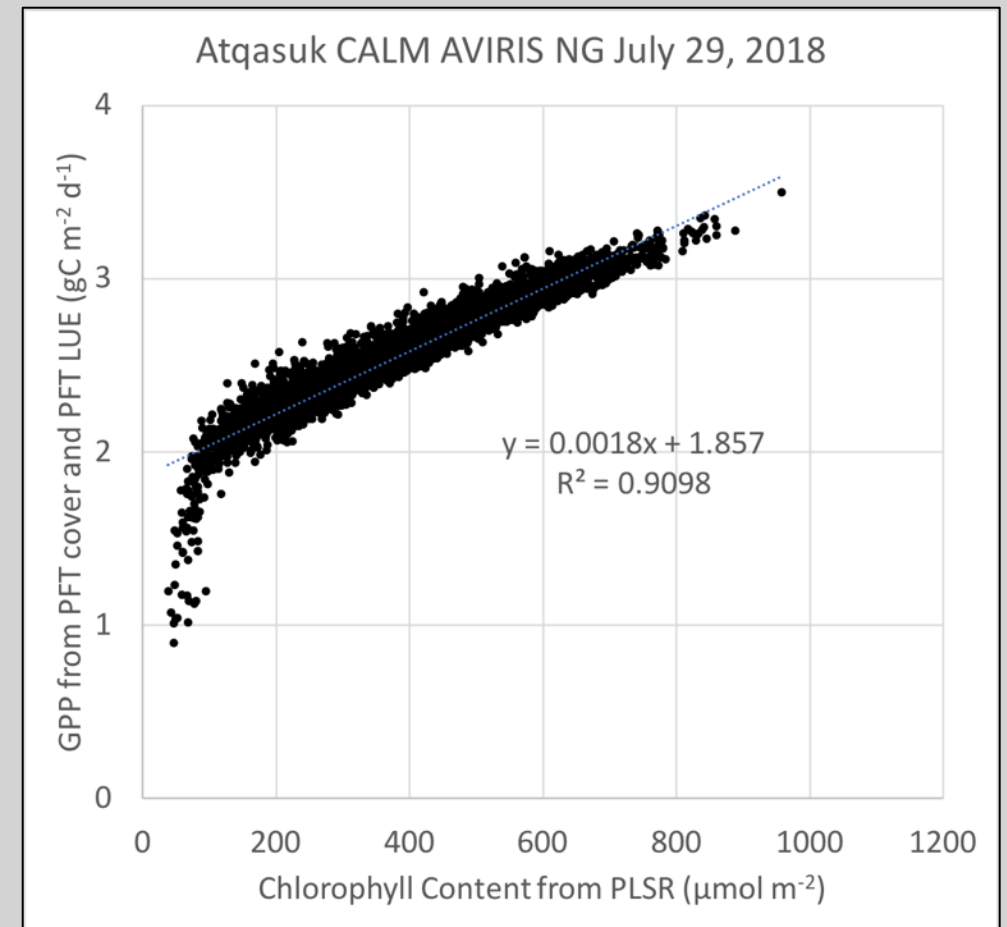
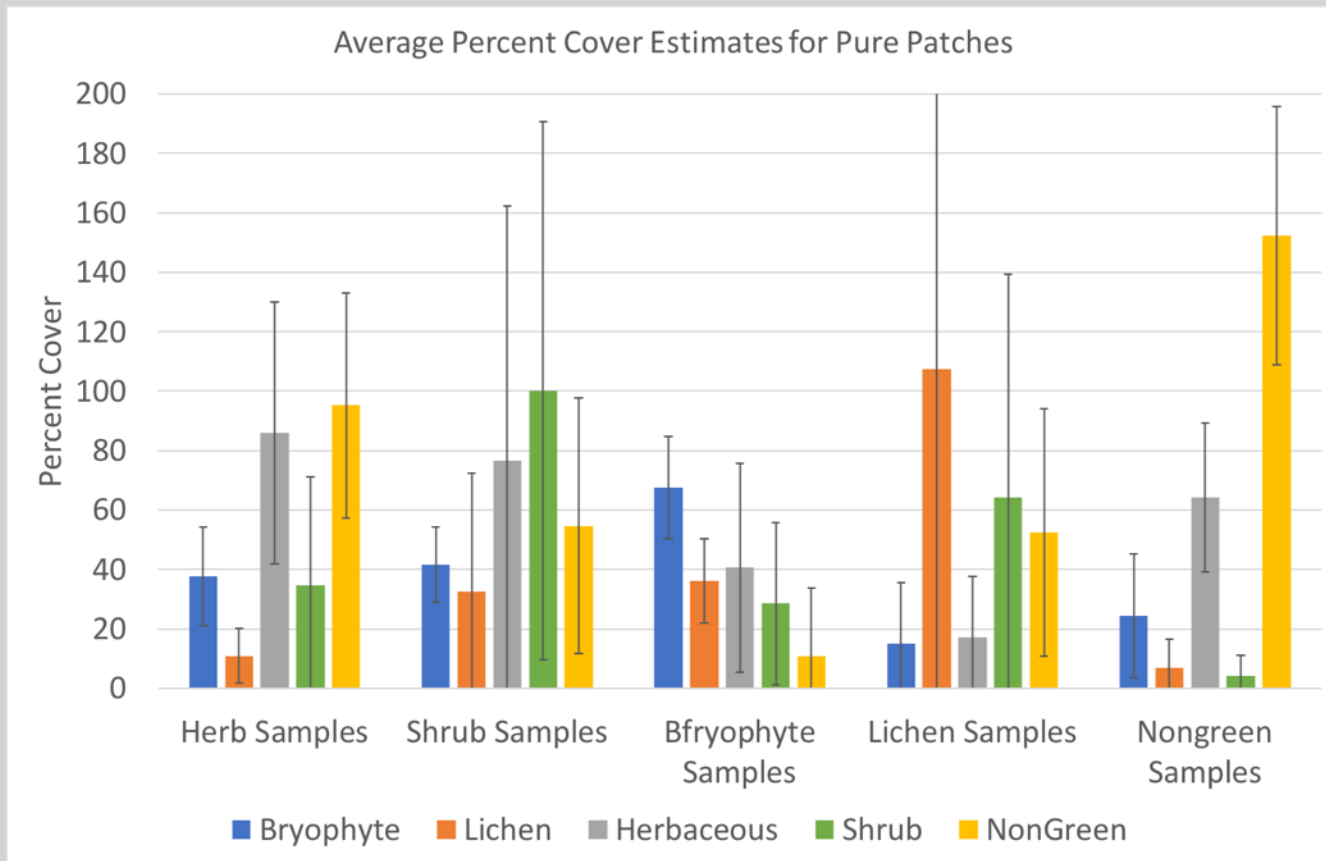
Atqasuk AVIRIS-NG July 29, 2018



Huemmrich, K.F., Campbell, P., Tweedie, C., Vargas, S., Hollister, R., Carroll, M., Gamon, J., and Oberbauer, S. Hyperspectral Mapping of Tundra Vegetation, *Env. Res. Comm.* *In review.*

K.F. Huemmrich, S.A. Vargas Z., C. Tweedie, P.K. Campbell, E. Middleton, NNX17AC58A Causes and Consequences of Arctic Greening: The Importance of Plant Functional Types

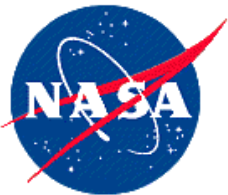
- Functional types rarely occur as pure pixels; challenges for endmembers
- Chlorophyll content strongly predicts PFT-based GPP (from LUE model)





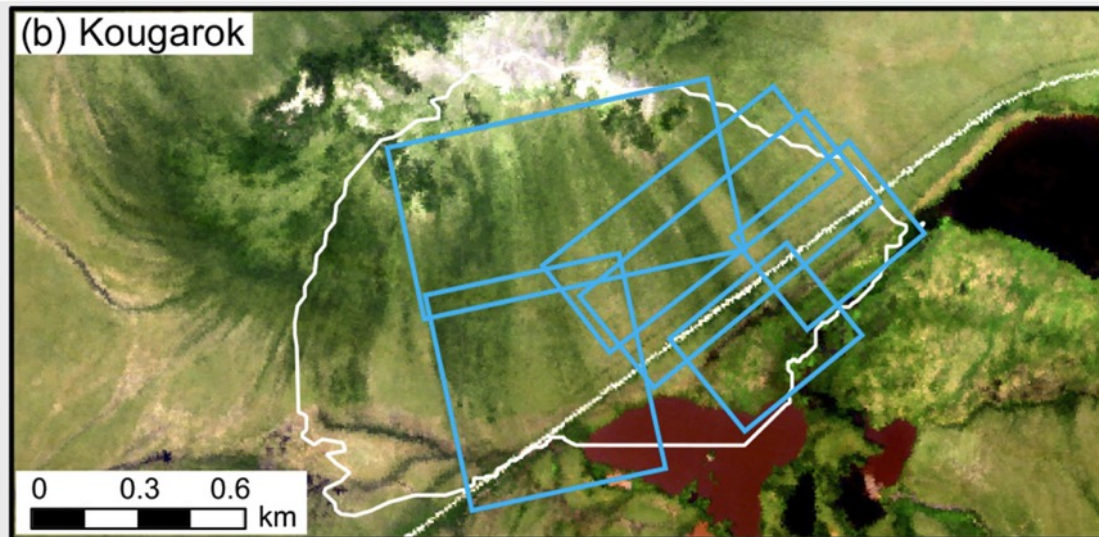
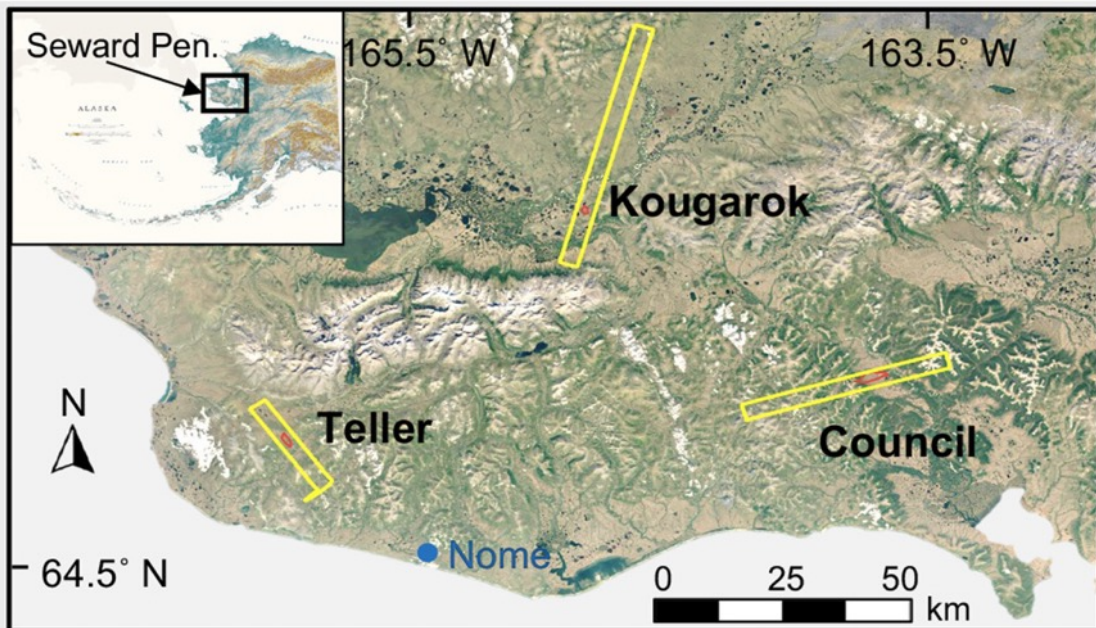
Scaling Fractional Cover (shrubification)

- ABoVE and NGEA-Arctic collaborate to study the drivers of tall shrub species distribution & expansion in low-Arctic using AVIRIS-NG
- Daryl Yang, Shawn Serbin (Brookhaven National Lab) + collaborators
- <https://doi.org/10.1016/j.rse.2022.113430>

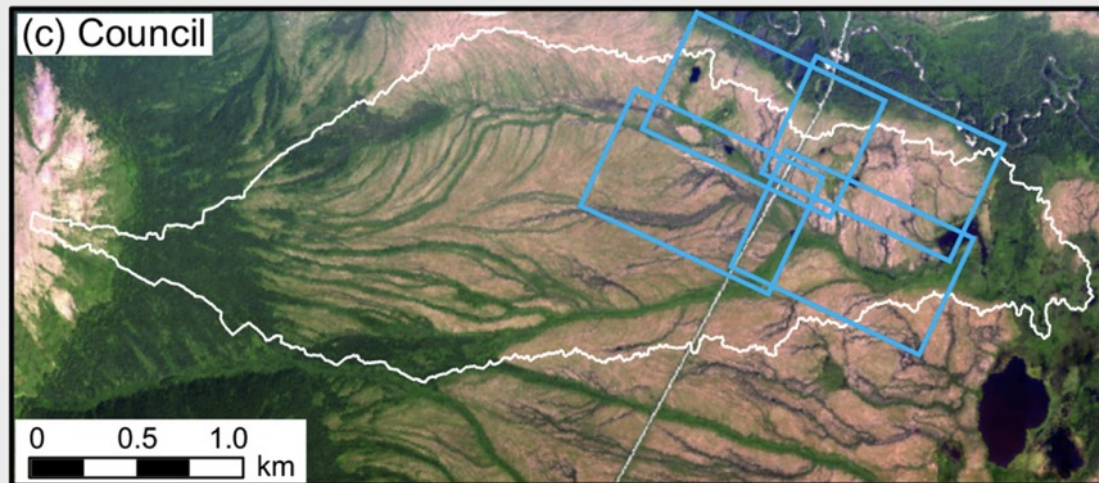


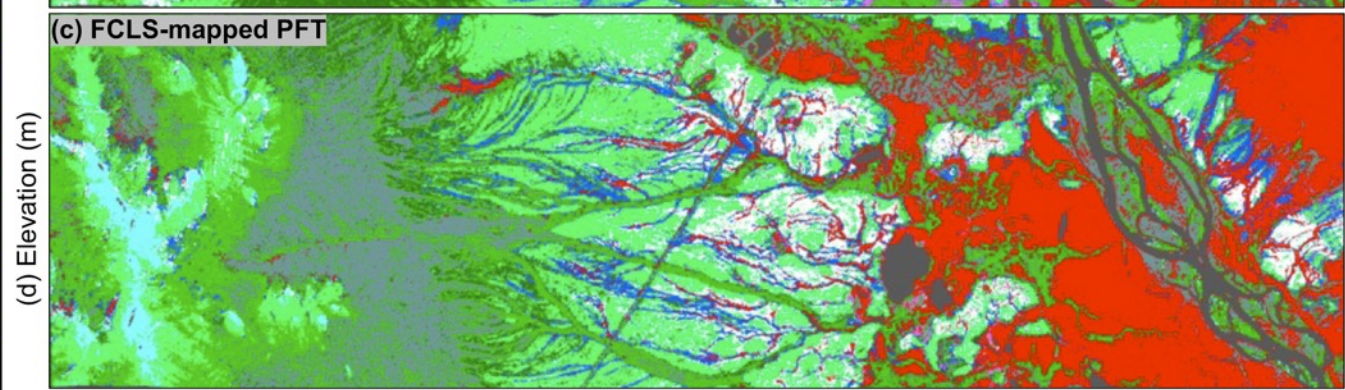
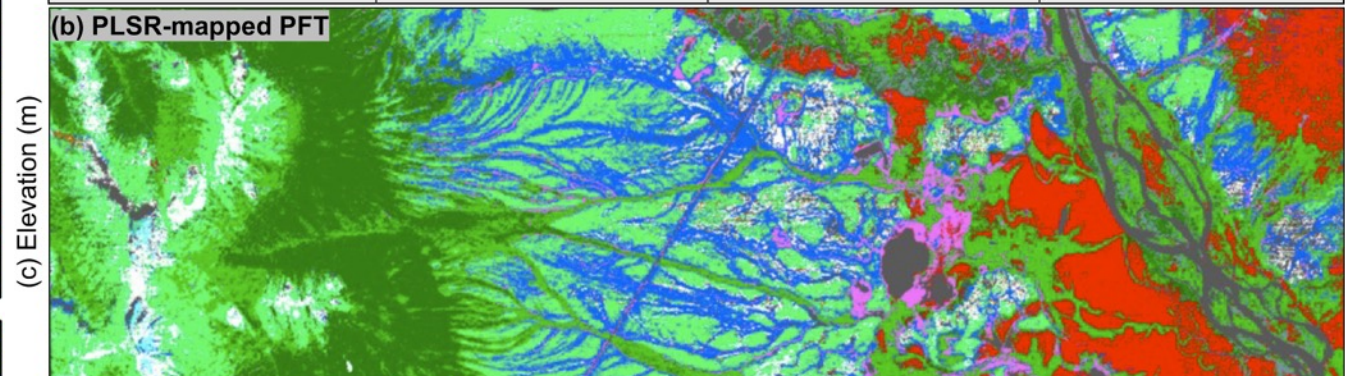
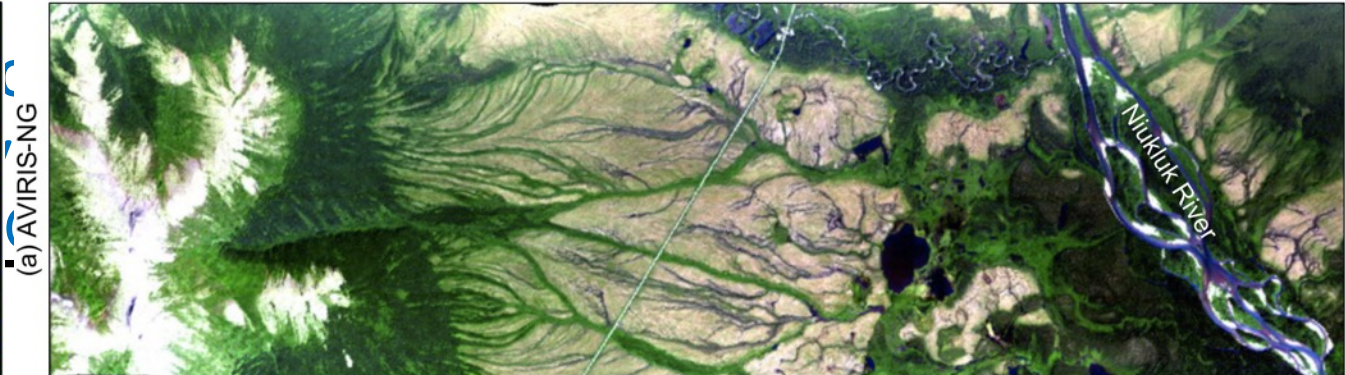
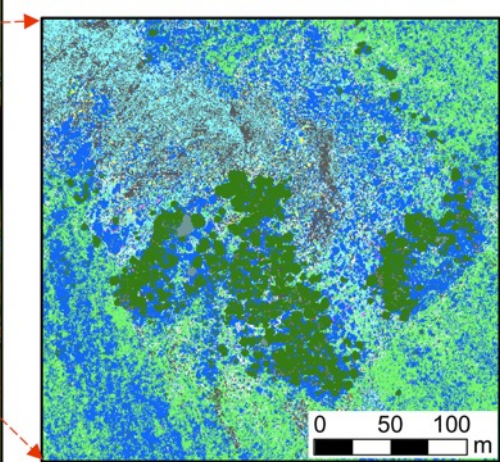
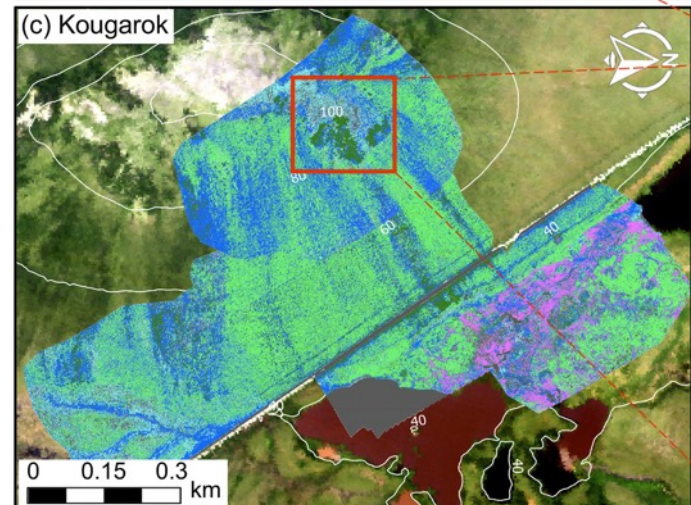
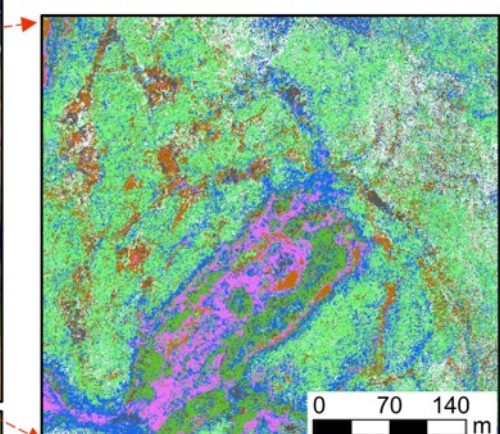
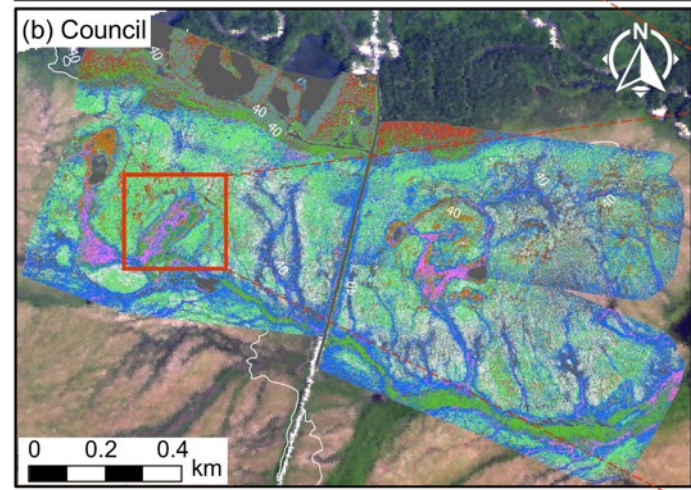
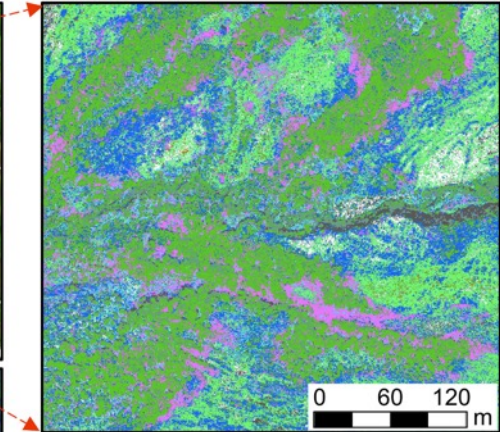
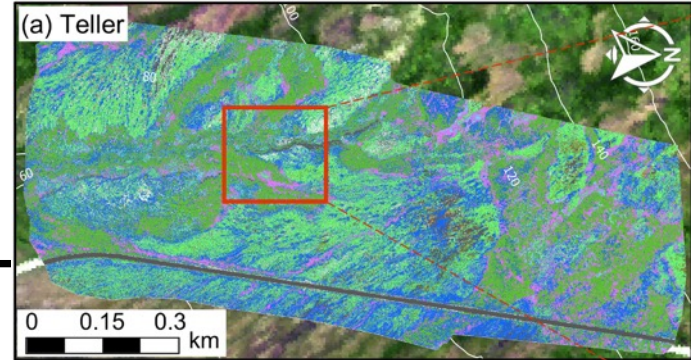
Integrating very-high-resolution UAS data and AVIRIS-NG imaging spectroscopy to map Arctic PFTs (NGEE-Arctic)

Yang *et al.* 2023, *Remote Sensing of Environment*

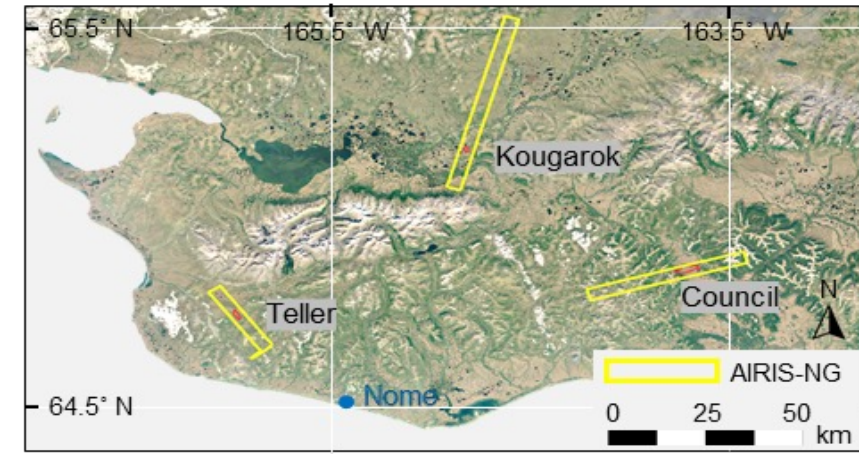
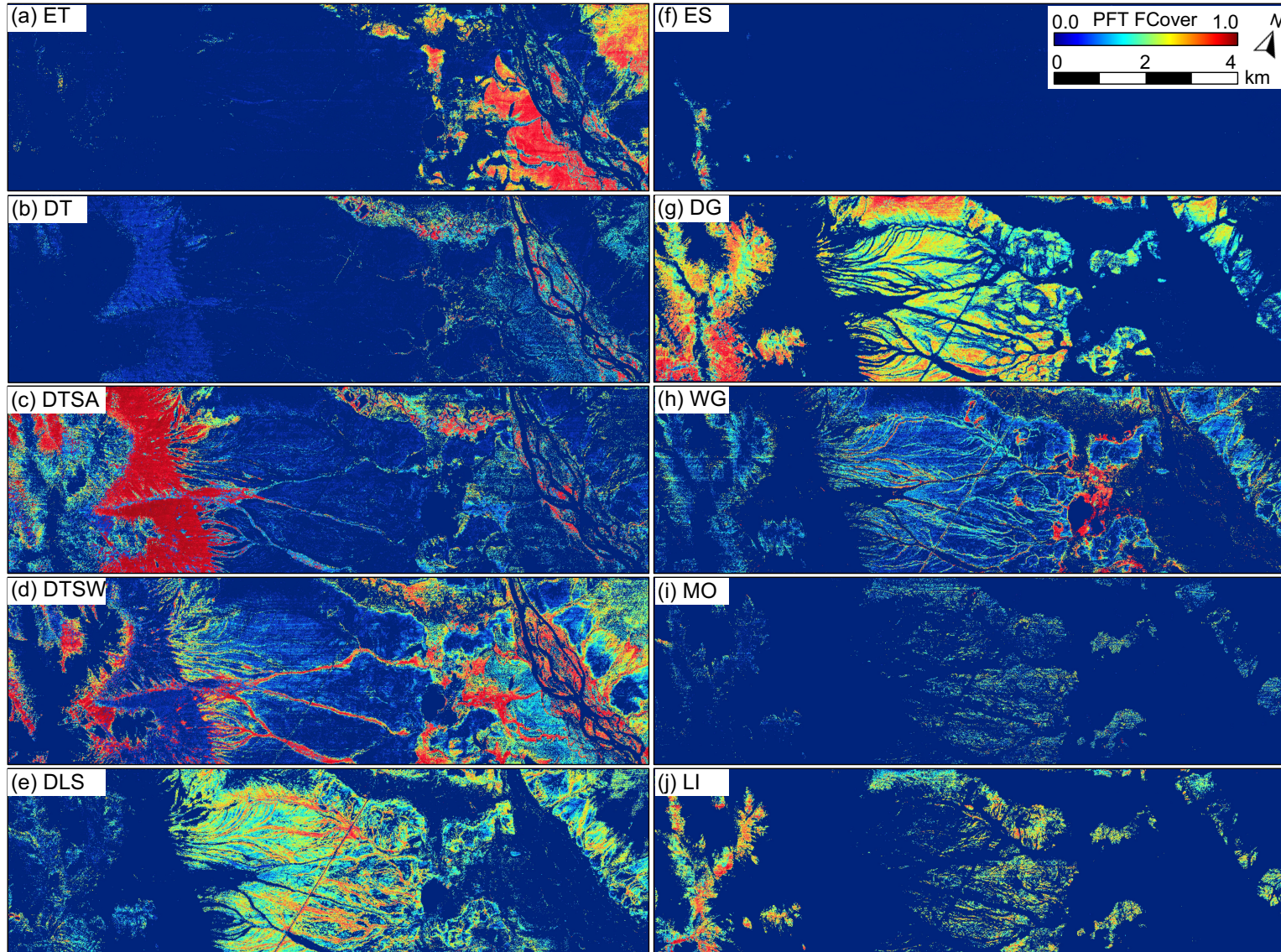


AVIRIS-NG UAS flights NGEE-Arctic watersheds





Combining UAS and AVIRIS-NG data to create regional-scale maps of Arctic tundra vegetation composition and fractional cover (example shown below, Council site on Seward Peninsula)

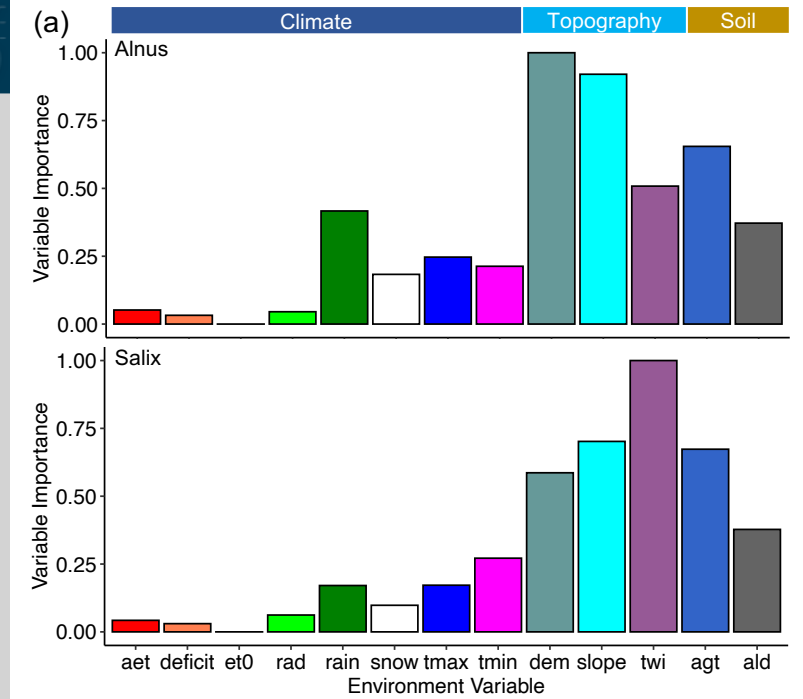


Findings:

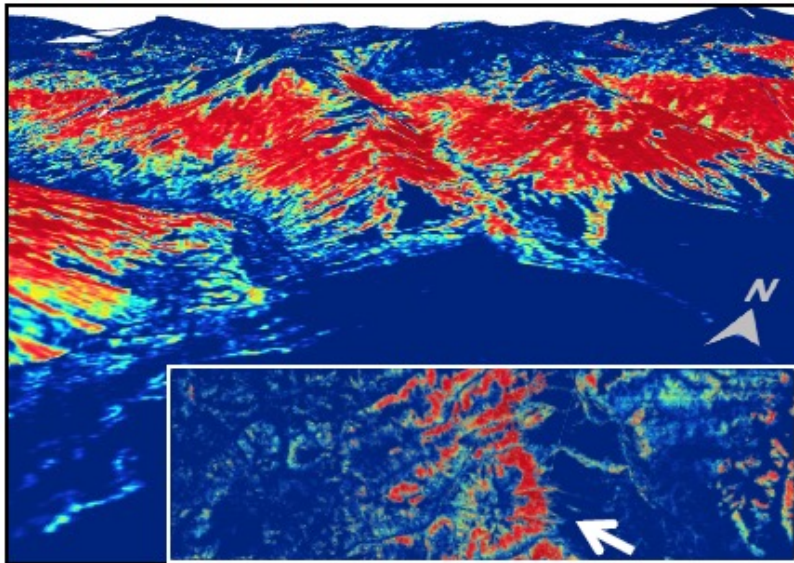
- The fractional cover of 12 Arctic PFTs are accurately captured with the UAS-based upscaling.
- The developed scaling method is highly capable of differentiating the composition of spectrally similar PFTs, e.g., alder, willow, and poplar trees.
- UAS-based upscaling is superior to traditional spectral mixing-based mapping of vegetation composition

Shrub expansion in the Arctic is limited by unfavorable abiotic or biotic factors.

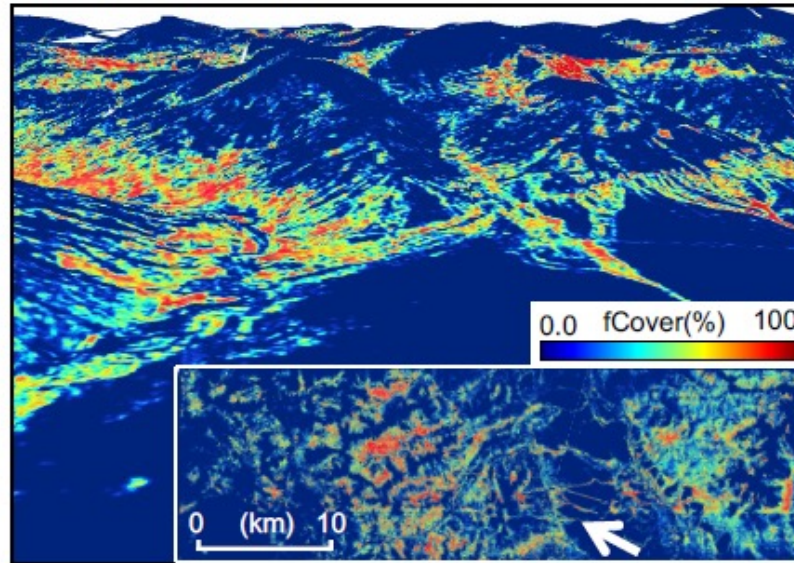
Topography-controlled processes (e.g., hydrology, snow distribution, and micro-scale disturbance) strongly control tall shrub expansion, but this control varies by species (e.g., alder and willow). **Alder moves uphill** and **willow expands along water resources down slope**.



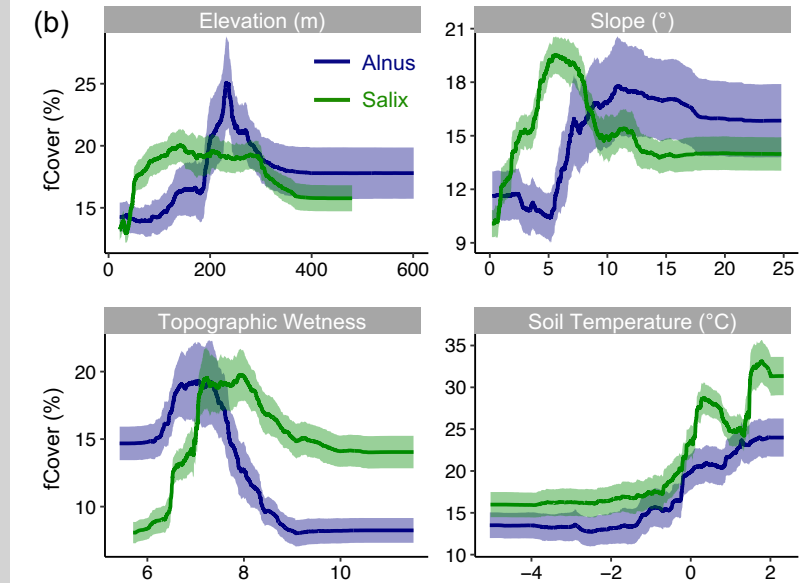
Alnus (DTSA) fCover



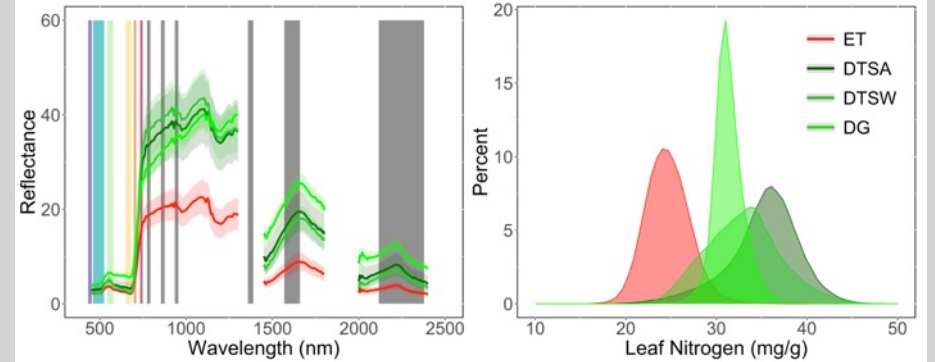
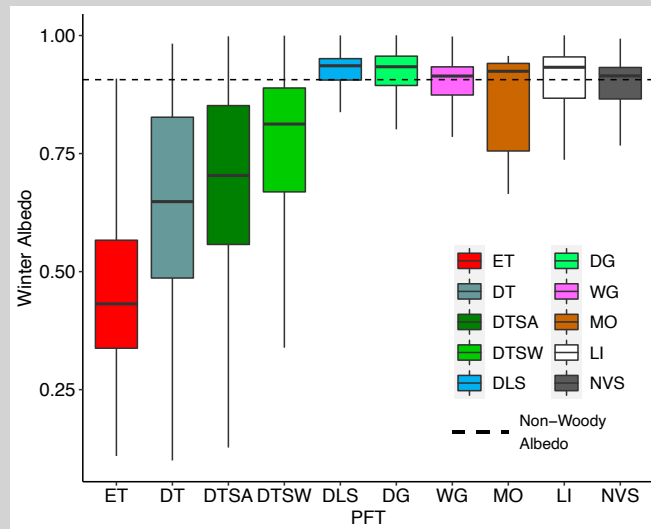
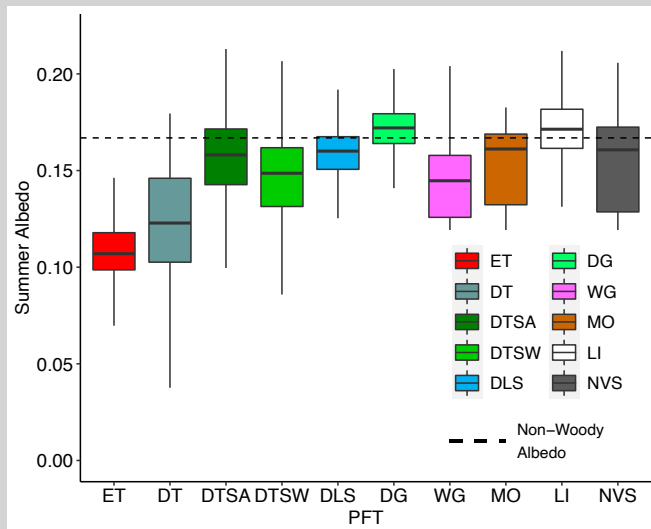
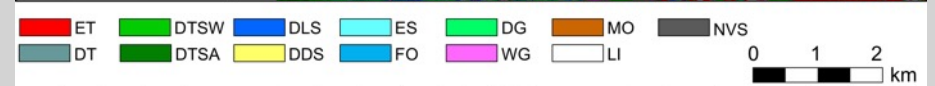
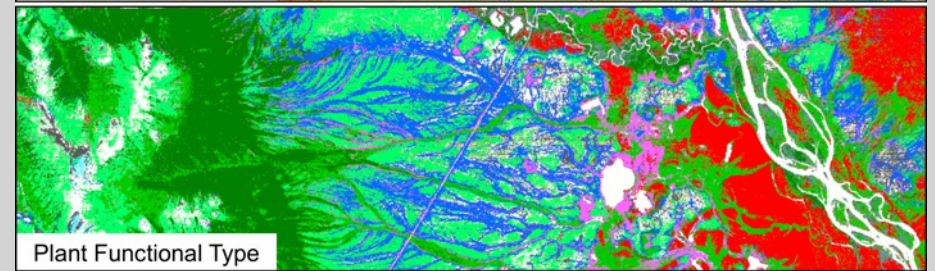
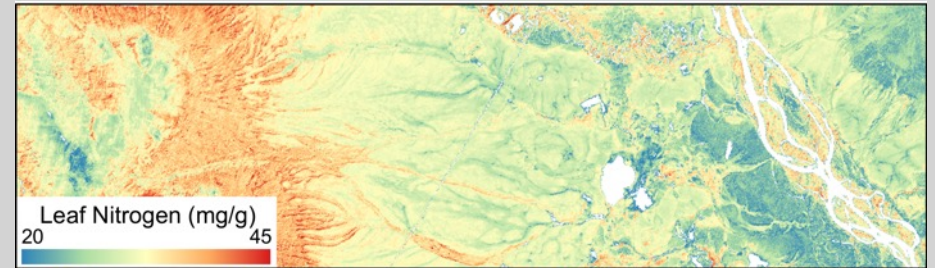
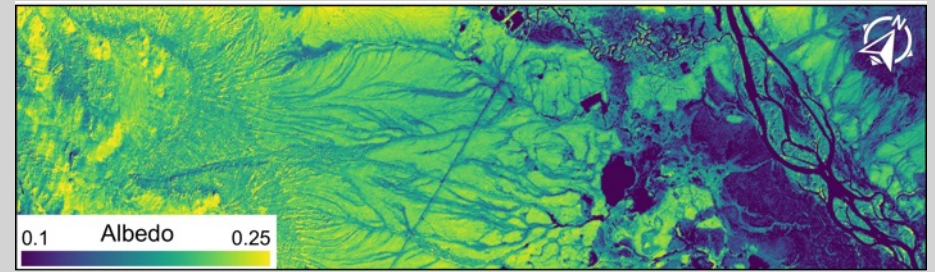
Salix (DTSW) fCover



Alnus and Salix fCover derived from AVIRIS-NG (Yang et al., 2023)



- A high spatial variation in canopy traits and albedo driven by vegetation composition
- Differences across PFTs imply that replacing other non-woody PFTs with tall shrubs will decrease winter-time albedo by **2-38%** and increase ecosystem nitrogen by up to **18%**.



Peter Nelson, Schoodic Institute at Acadia National Park

- Ground to UAV spectroscopy for transferrable mapping of plant functional types (PFTs) in the ABoVE domain
 - Map PFTs in 32 AVIRIS images using ground and UAV spectra to improve transfer across sites and imaging conditions
- What are in the dimensions of AVIRIS ABoVE data? Team paper leading towards scaling efforts (see Spectroscopy WG presentation)

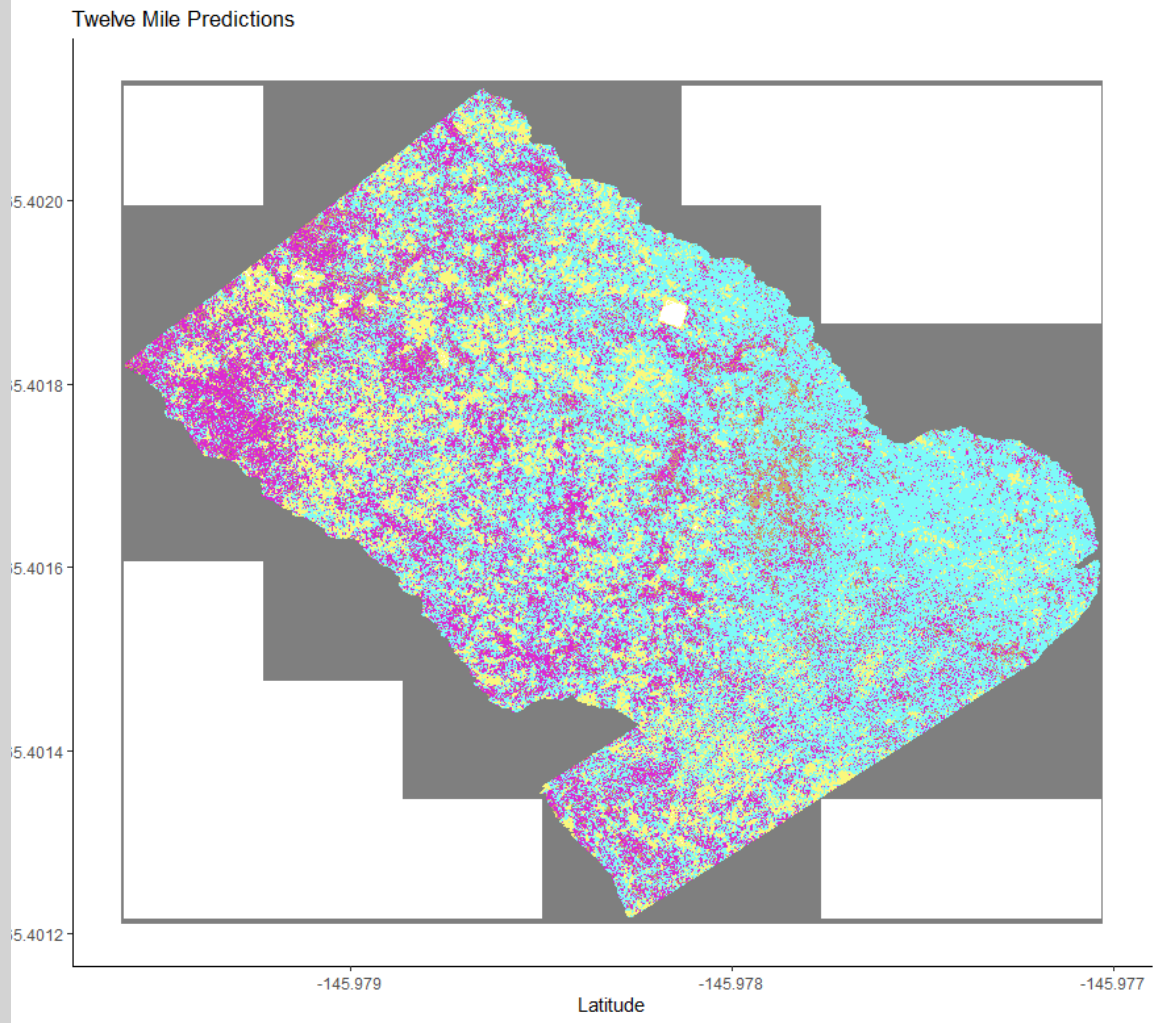
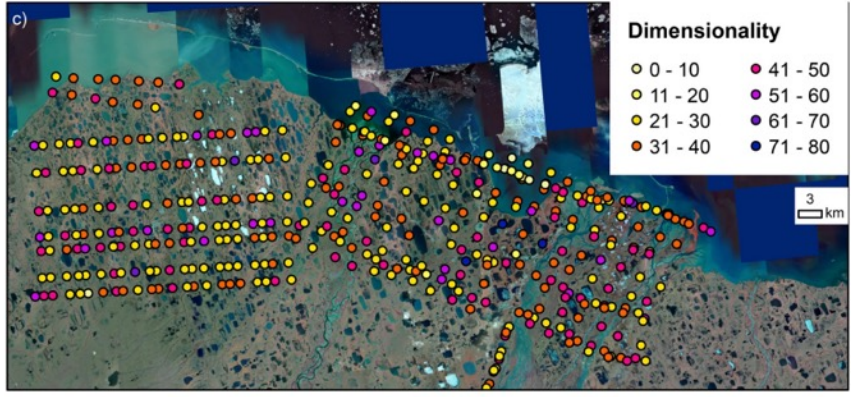
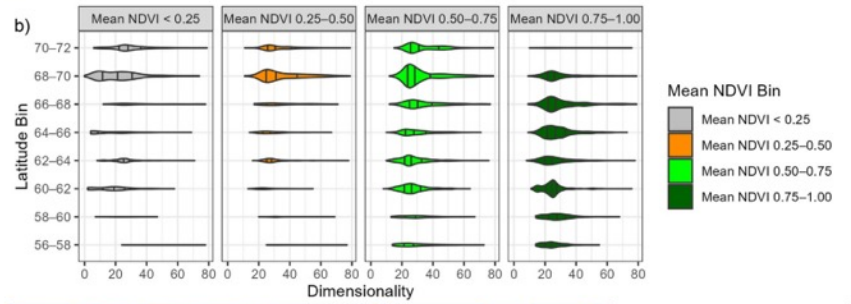
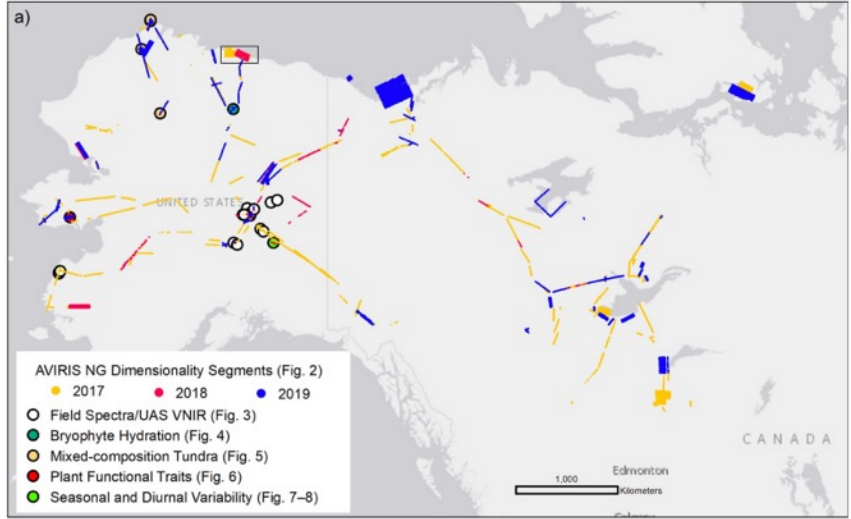
JGR Biogeosciences

RESEARCH ARTICLE
10.1029/2021JG006697

Special Section:
The Earth in living color: spectroscopic and thermal imaging of the Earth: NASA's Decadal Survey Surface Biology and Geology Designated Observable

Remote Sensing of Tundra Ecosystems Using High Spectral Resolution Reflectance: Opportunities and Challenges

Peter R. Nelson¹, Andrew J. Maguire², Zoe Pierrat³, Erica L. Orcutt⁴, Dedi Yang⁵, Shawn Serbin⁶, Gerald V. Frost⁶, Matthew J. Macander⁶, Troy S. Magney⁴, David R. Thompson², Jonathan A. Wang⁷, Steven F. Oberbauer⁸, Sergio Vargas Zesati⁹, Scott J. Davidson^{10,11}, Howard E. Epstein¹², Steven Unger⁸, Petya K. E. Campbell¹³, Nimrod Carmon², Miguel Velez-Reyes⁹, and K. Fred Huemmrich¹³



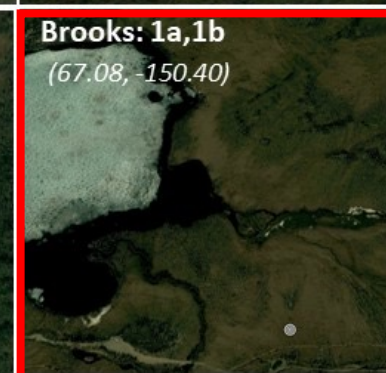
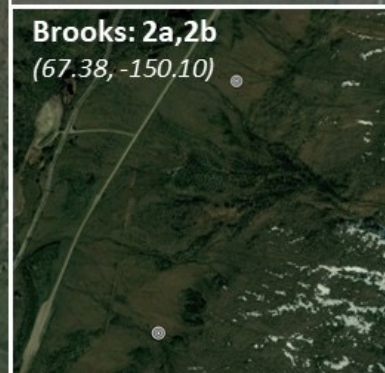
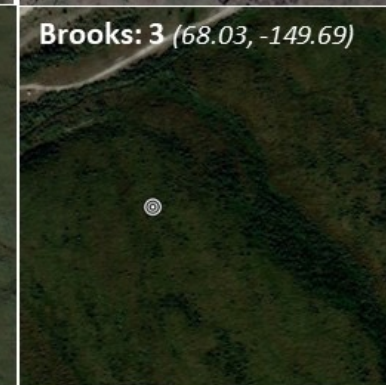
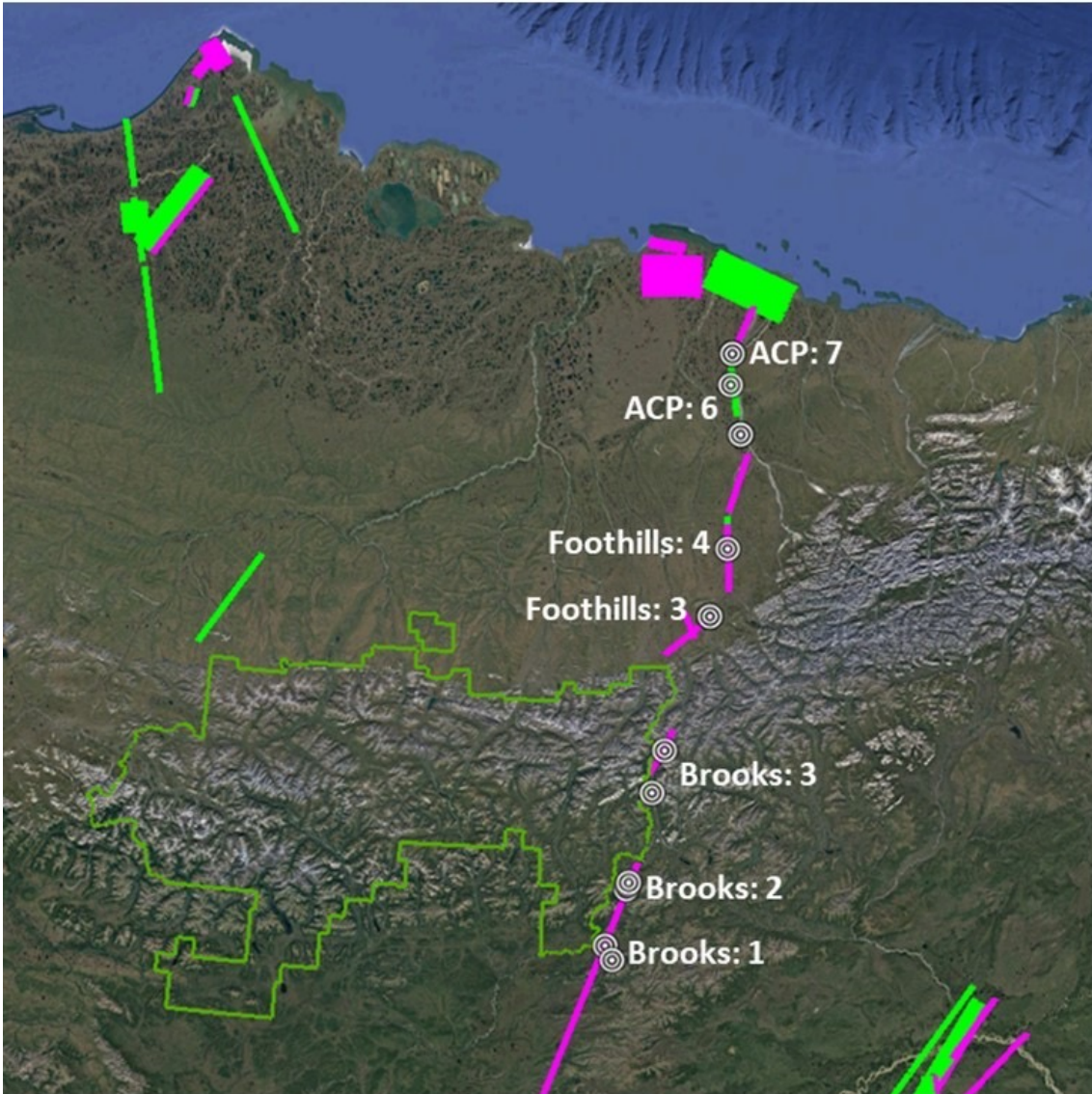
Key Result: Coupling ground and UAV-based spectra for PFTs with AVIRIS reflectance enables subpixel fractional cover estimation.



Wenqu Chen, Mark Lara and Jennifer Fraterrigo (University of Illinois)

- Multiscale Mapping of Tundra Plant Traits Using Hyperspectral Data from UAS and AVIRIS-NG
- Testing optimal plant trait scaling approach across overlapping Airborne Visible Infrared Imaging Spectrometer-Next Generation (AVIRIS-NG) flight lines (ground to UAS to AVIRIS-NG).
- Department of Energy, Grant DE-SC0021094

Multiscale Mapping of Tundra Plant Traits Using Hyperspectral Data from UAS and AVIRIS-NG



Data from site 1B shown on next slides

Plant Trait Data Collection

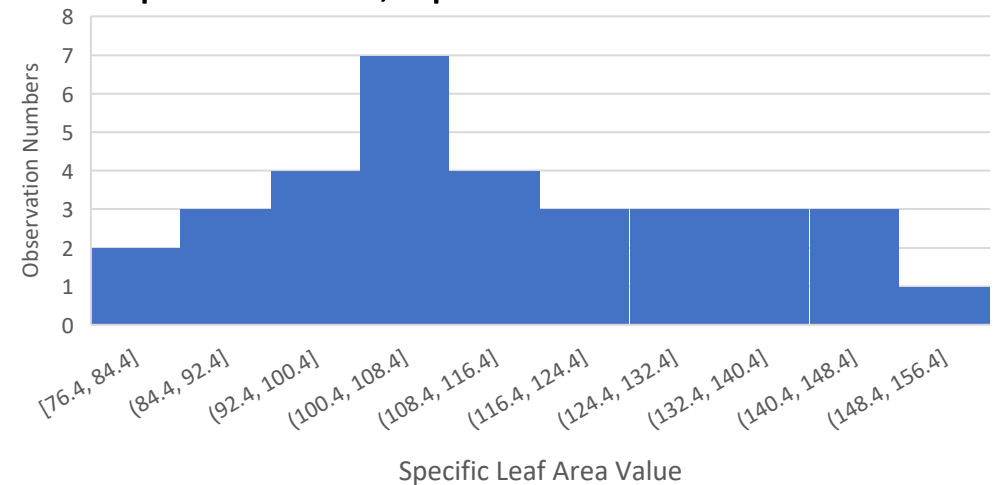


Measured above and below ground plant traits include:

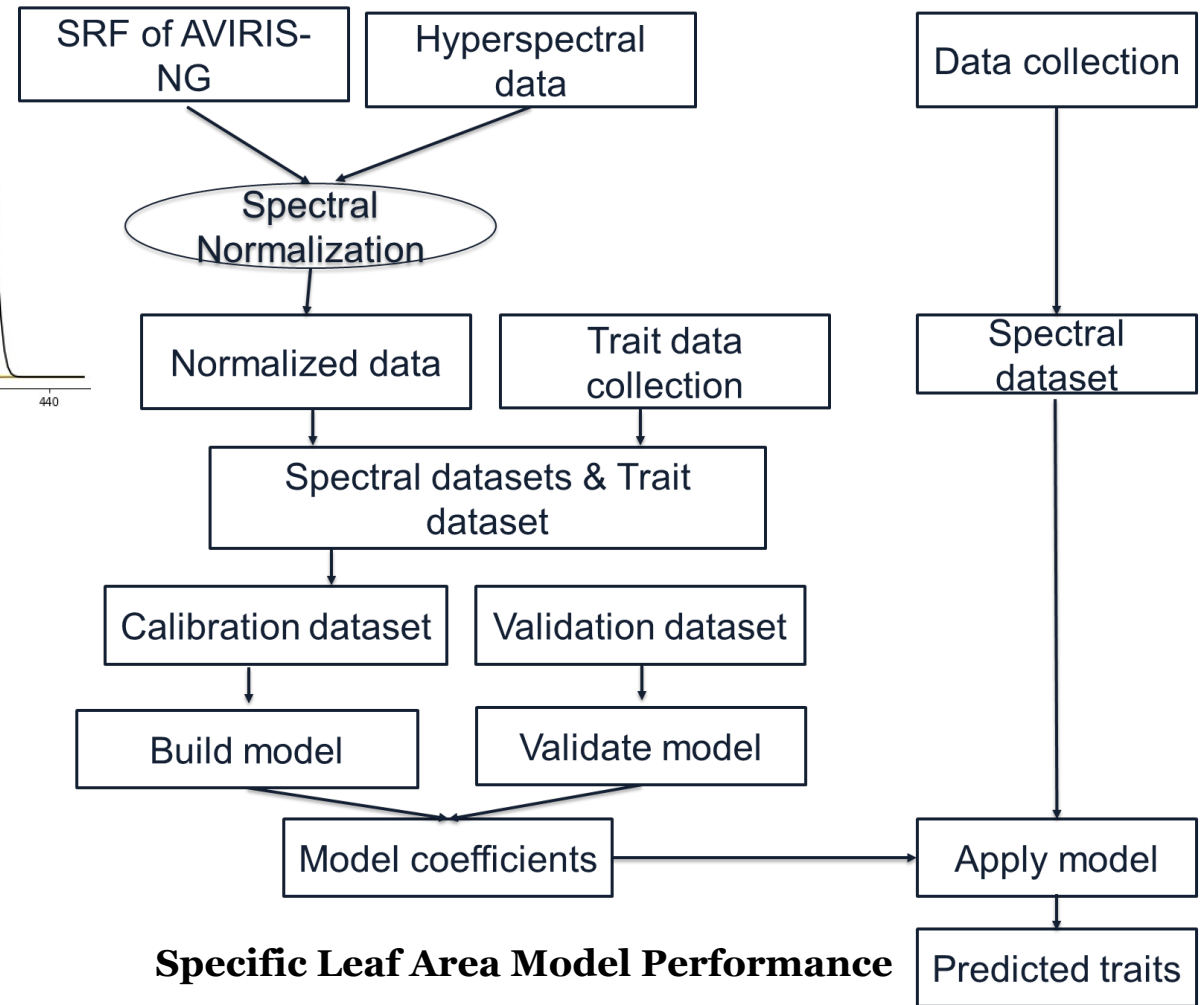
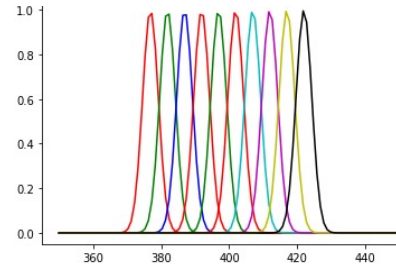
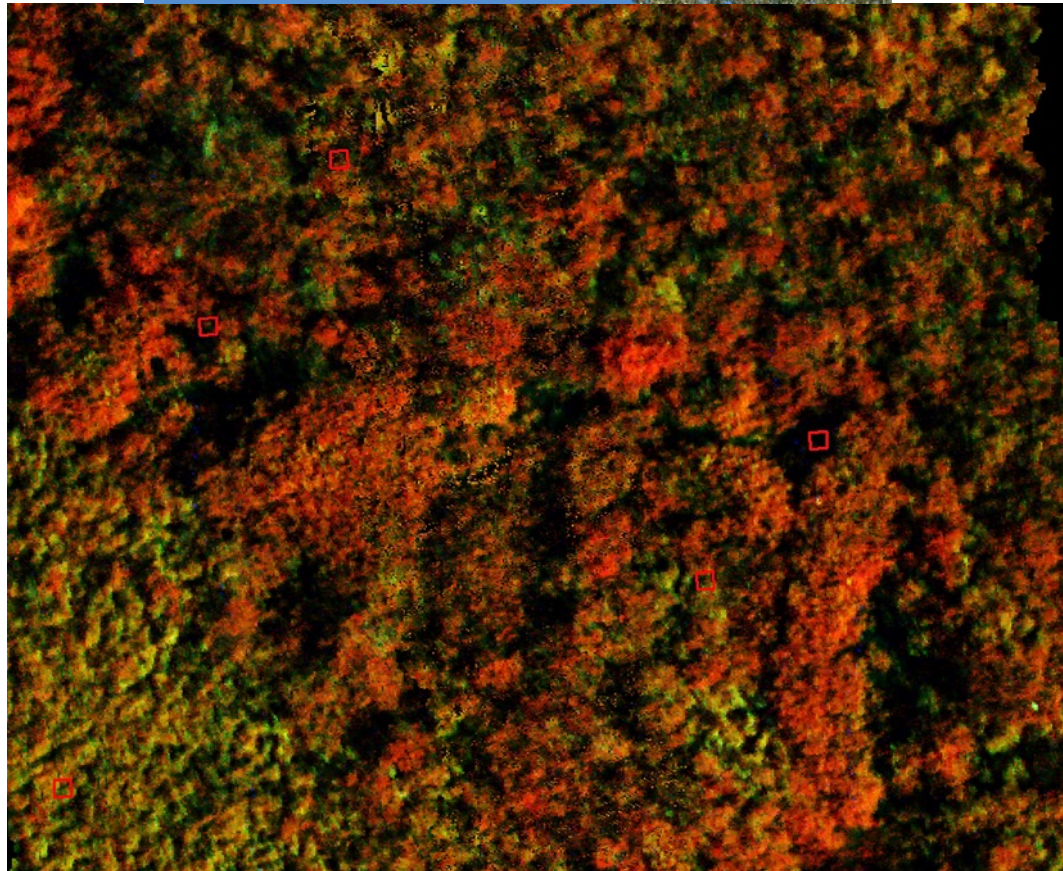
- Specific leaf area (SLA)
- Leaf dry matter content
- Leaf N and $\delta^{15}\text{N}$ (N source)
- Leaf $\delta^{13}\text{C}$ (plant water stress)
- Height
- Specific root length (SRL)
- Root tissue density
- Root N and $\delta^{15}\text{N}$
- Mycorrhizal colonization



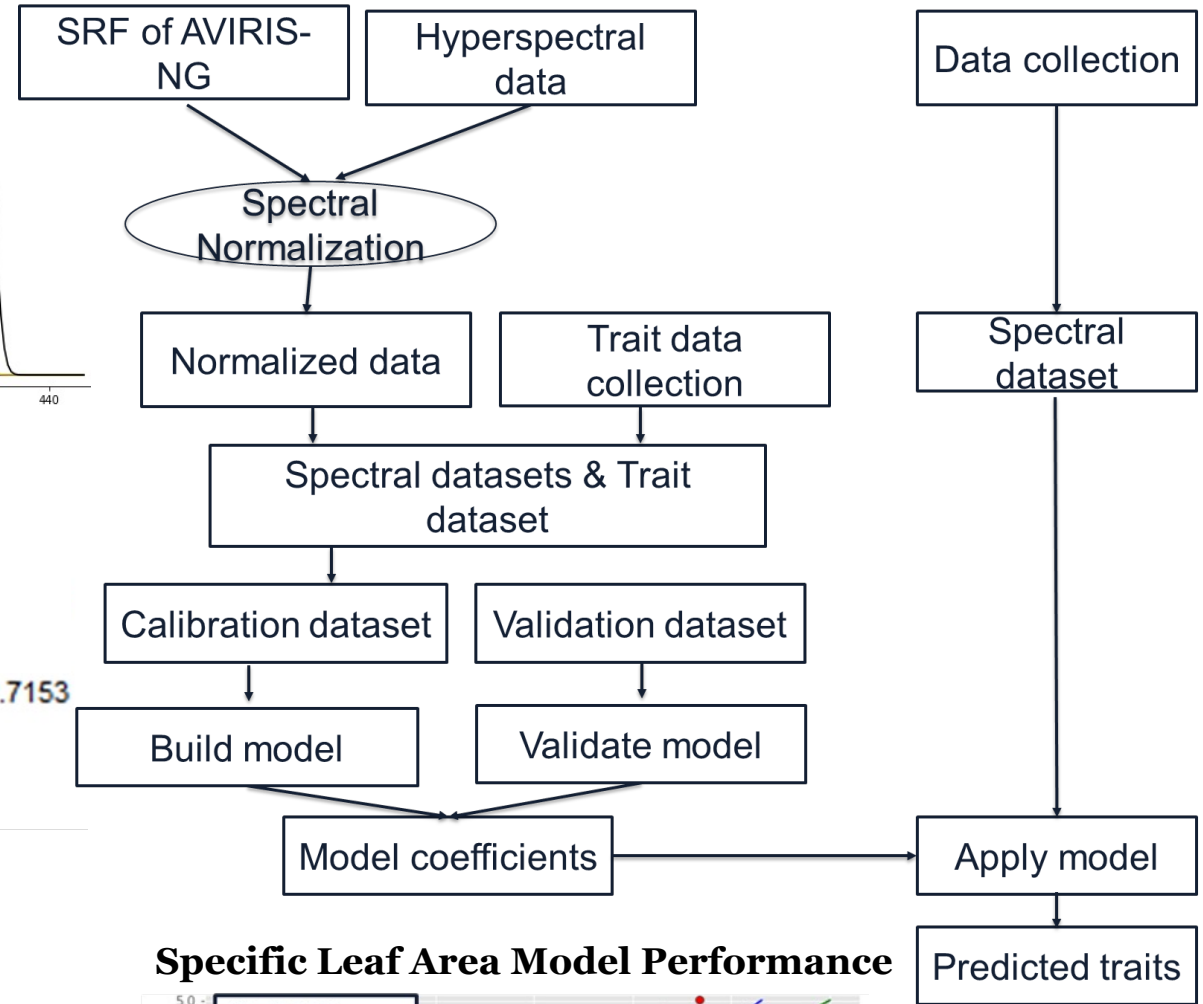
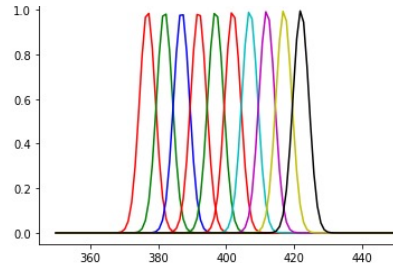
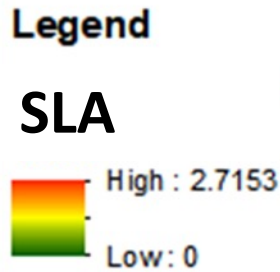
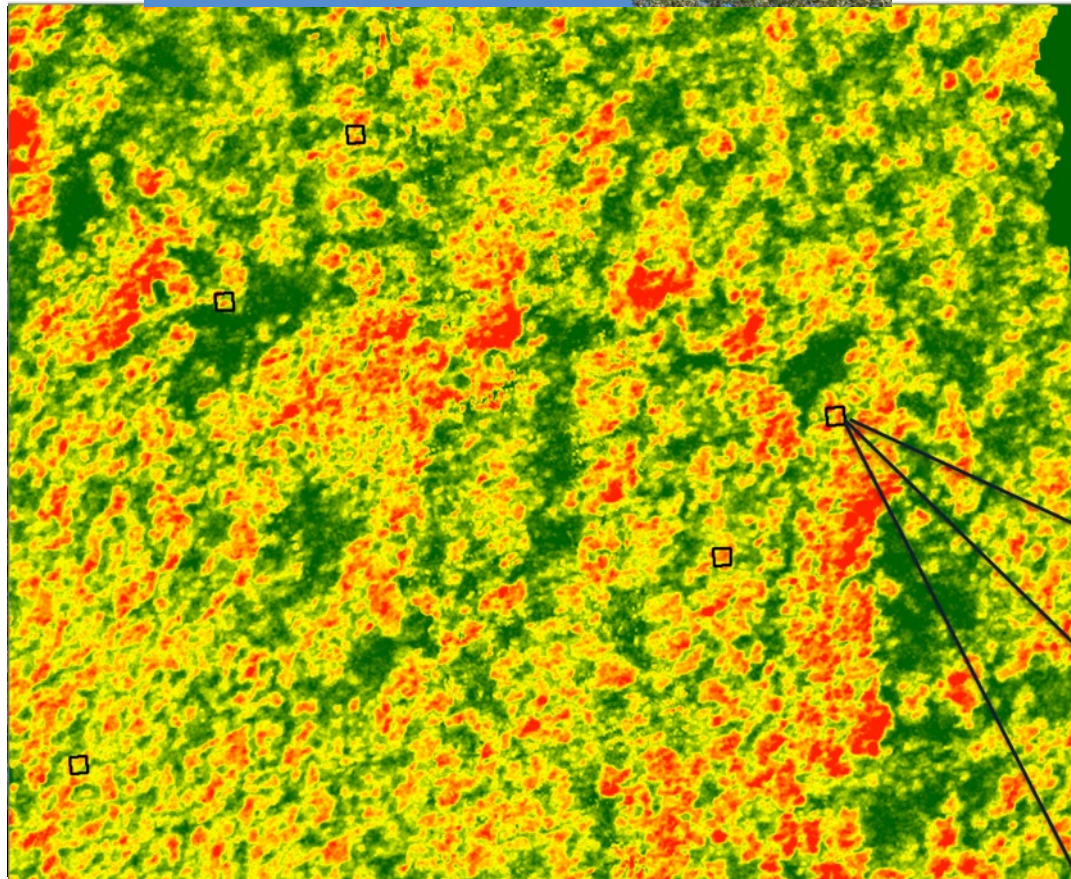
Example: Site 1B, Specific Leaf Area Data



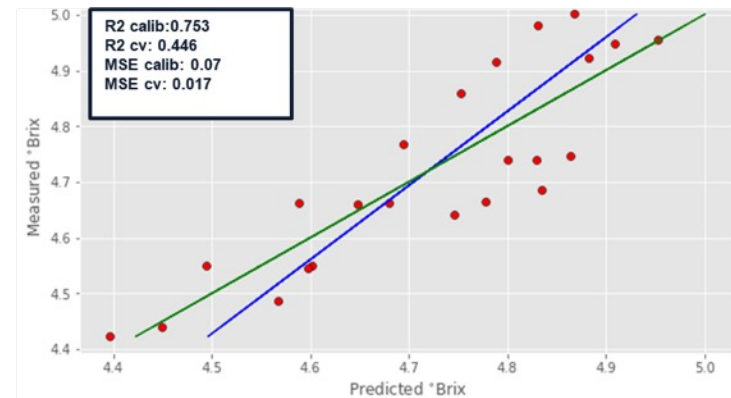
Plant Trait Mapping and Upscaling

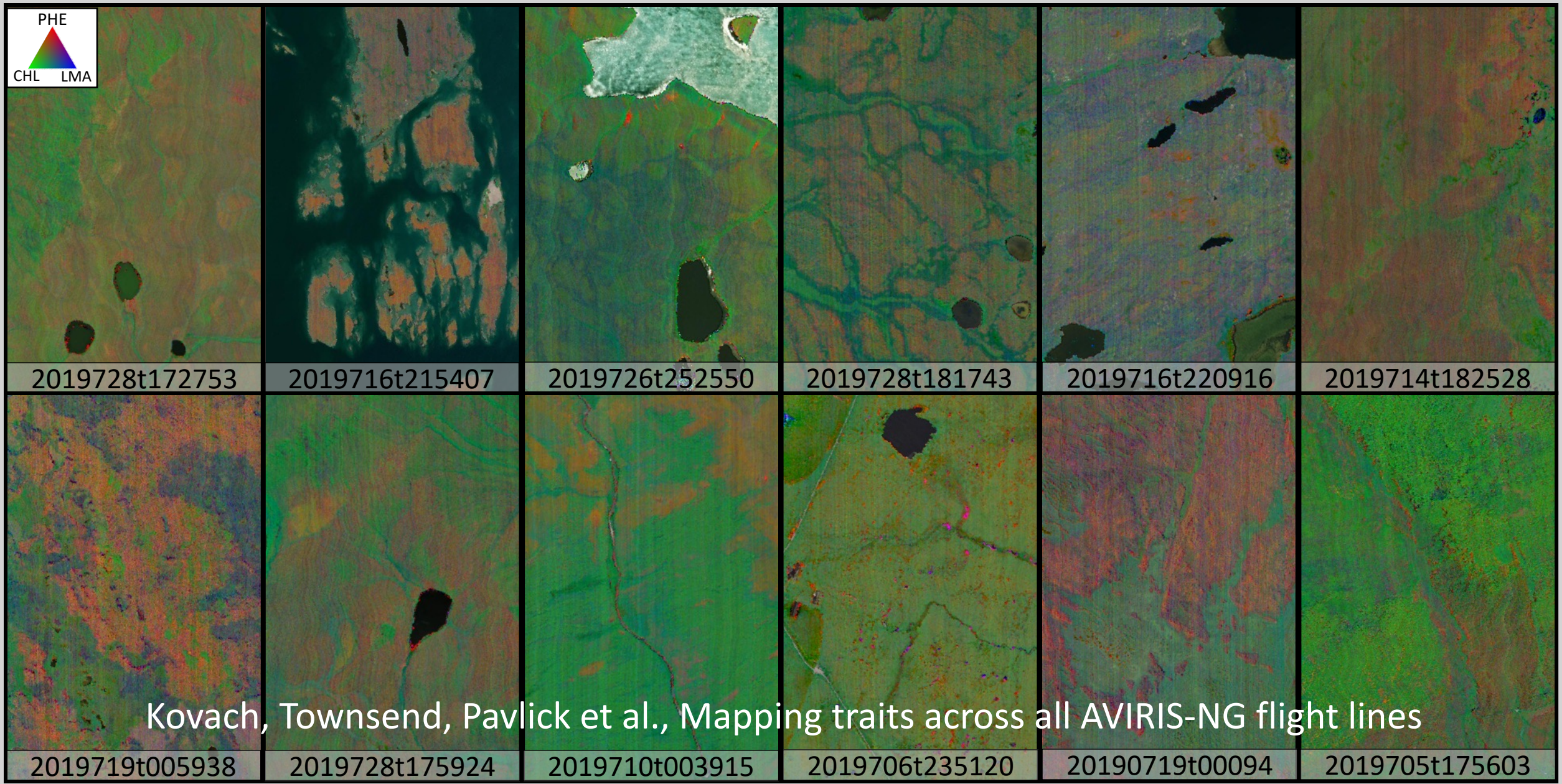


Plant Trait Mapping and Upscaling



Specific Leaf Area Model Performance

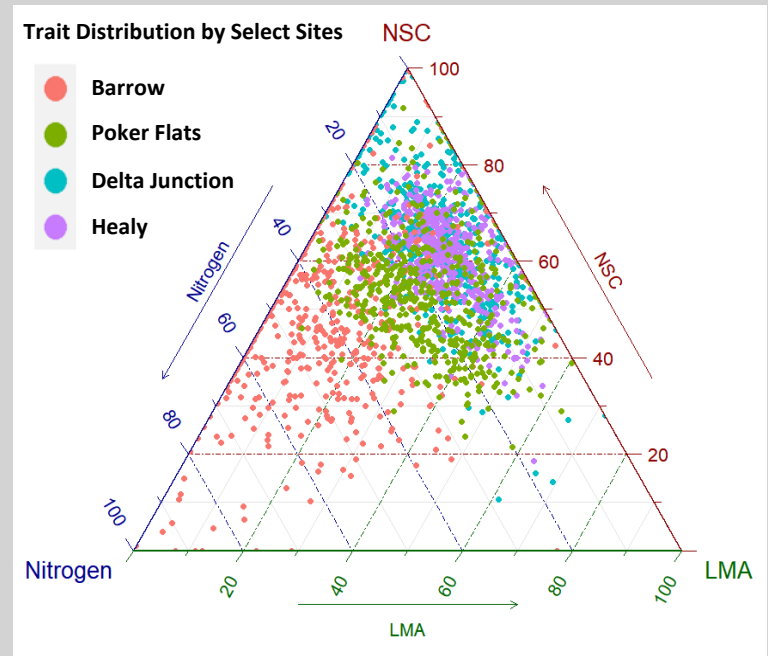
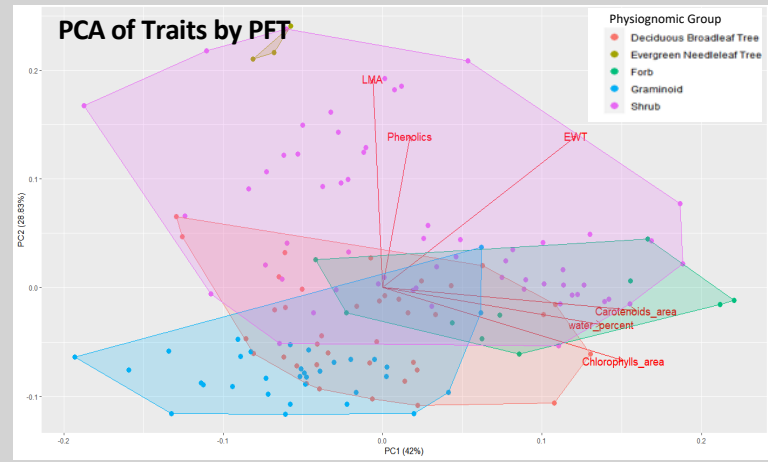
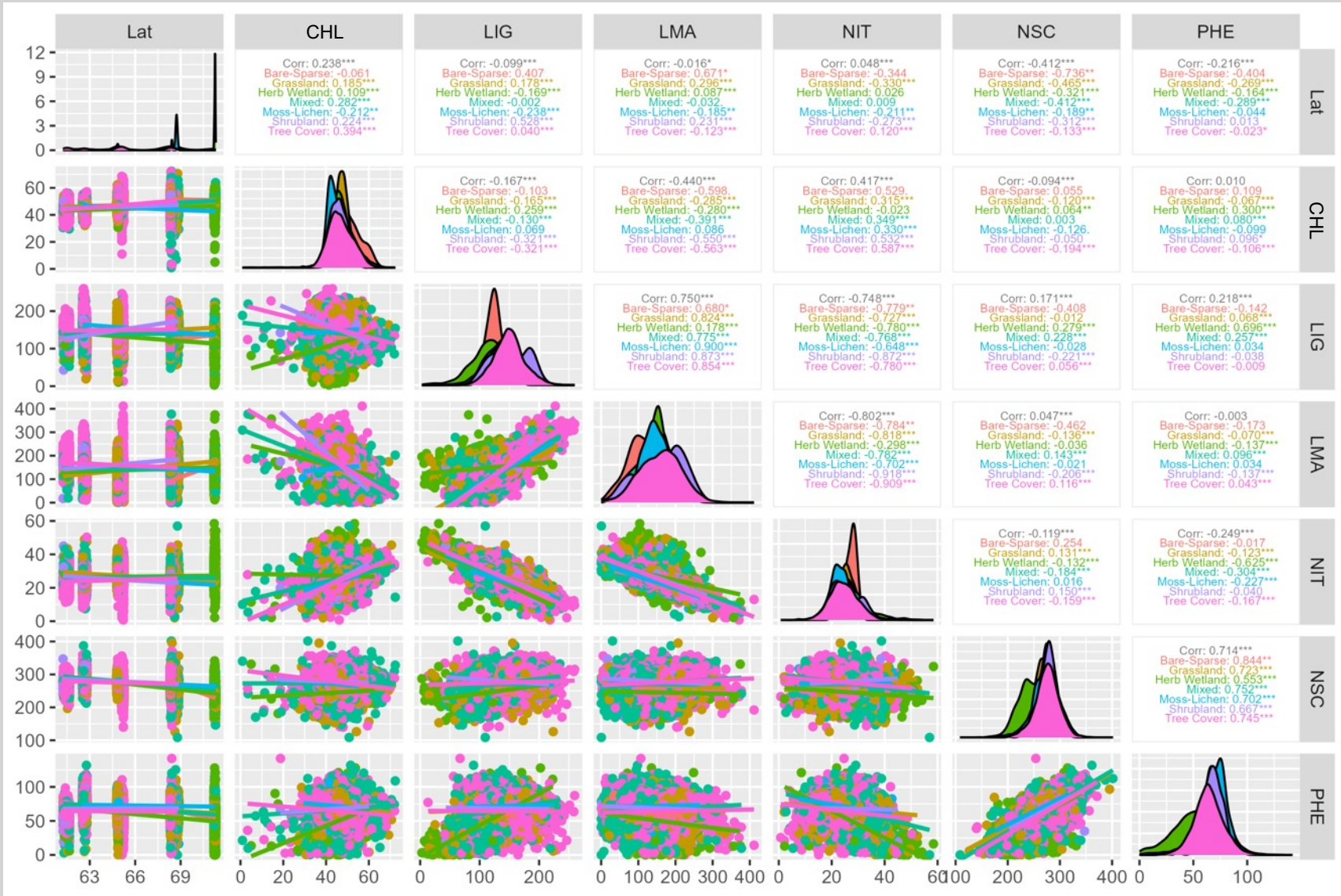




Kovach, Townsend, Pavlick et al., Mapping traits across all AVIRIS-NG flight lines



Trait Relationships and Distributions Across ABoVE Domain, within PFT Variation



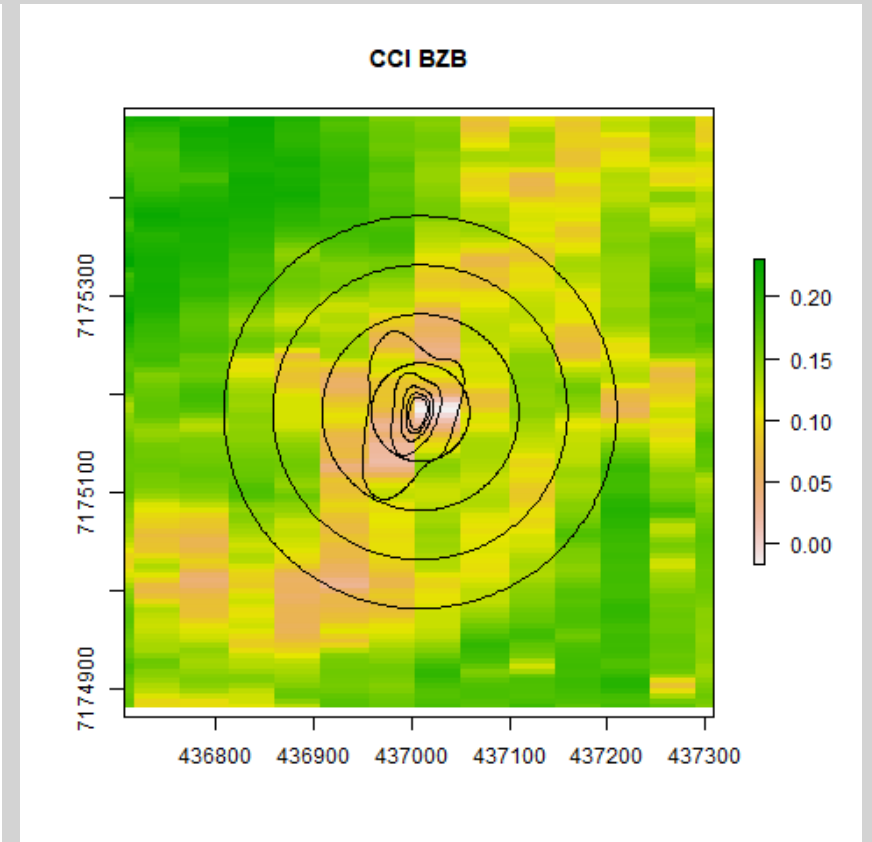
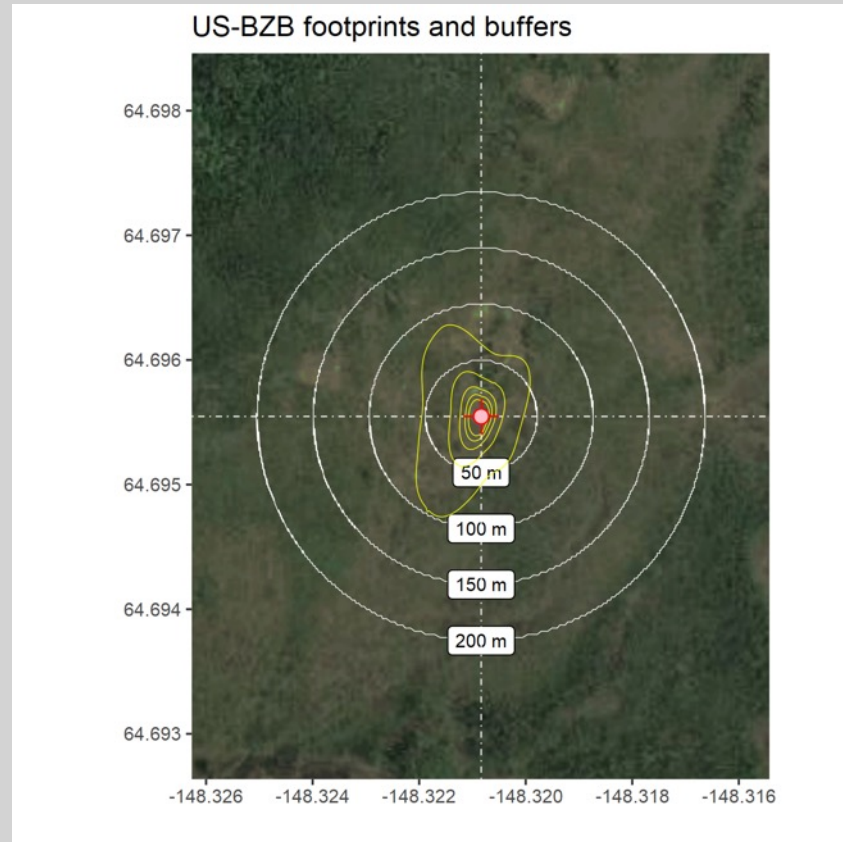


Linkage to Flux Towers

- Erica Orcutt (Sacramento State), Troy Magney (UC-Davis), Christian Frankenburg (Caltech) + collaborators

Assessing the variability of aircraft remote sensing products (CFIS and AVIRIS-NG) within flux tower footprints

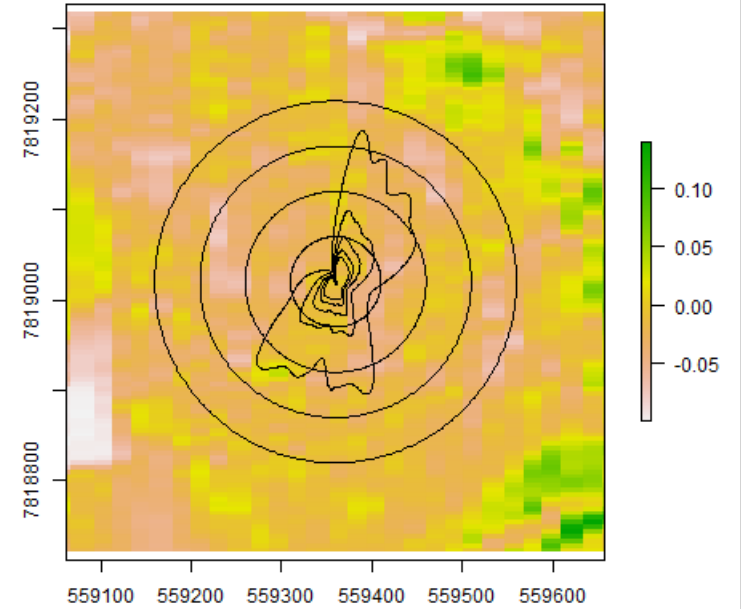
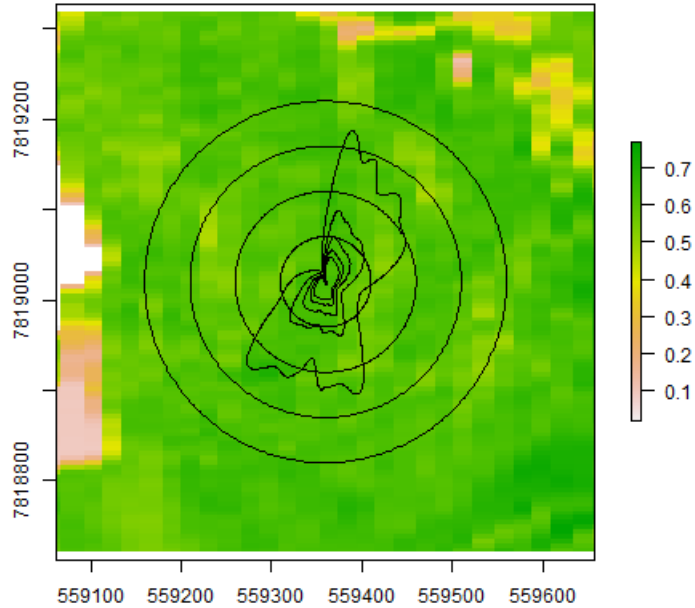
- Question: What is the hyperspectral variability around flux towers at 14 sites within ABoVE domain?
- Looked at both radii contours (50-200m) and weighted averages of flux tower footprints



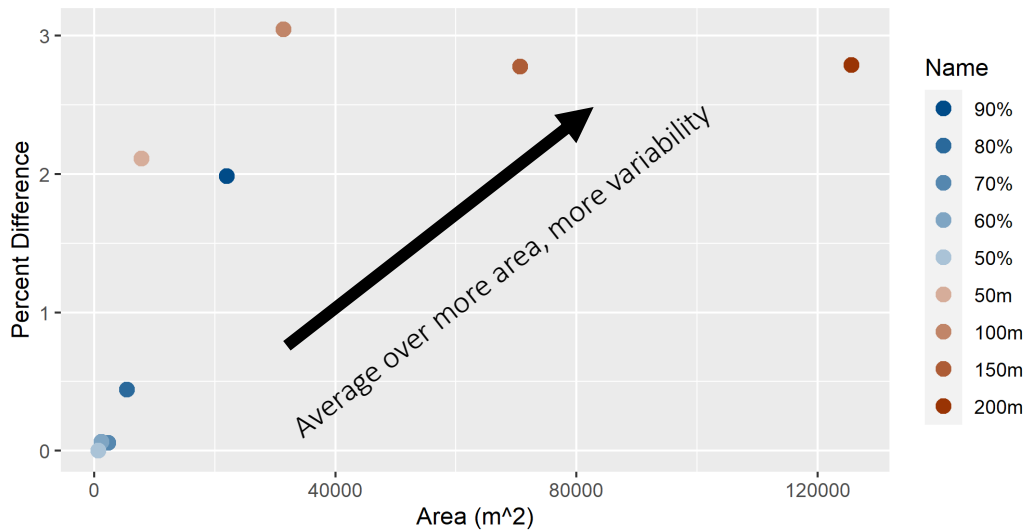
Erica L. Orcutt*, Christian Frankenberg, Housen Chu, Kyle A. Arndt, Eugenie S. Euskirchen, Gabriel Hould Gosselin, Manuel Helbig, Hiroki Ikawa, Hideki Kobayashi, Andrew J. Maguire, Philip Marsh, Gesa Meyer, Walter C. Oechel, Ryan Pavlick, William L. Quinton, Adrian V. Rocha, Christopher Schulze, Oliver Sonnentag, Donatella Zona, & Troy S. Magney

Atqasuk

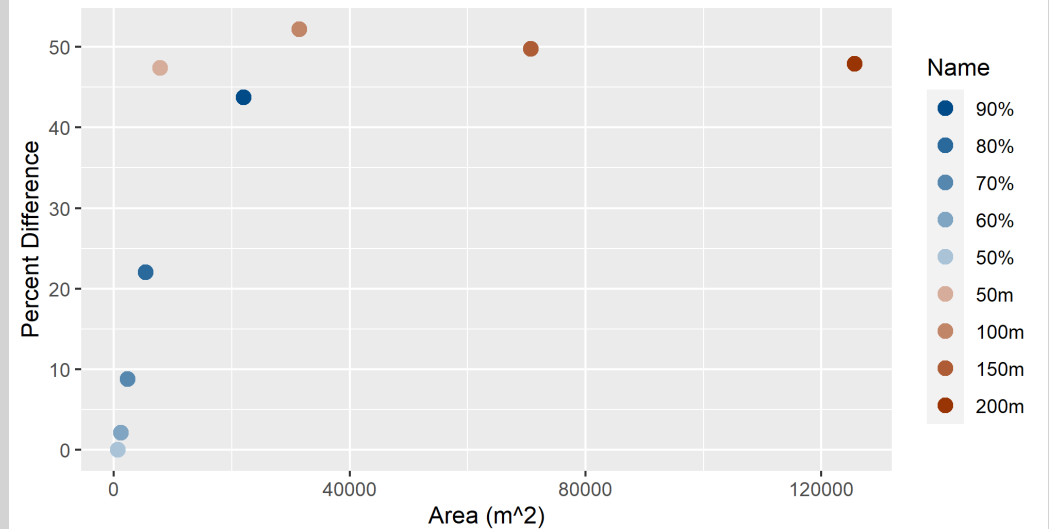
NDVI and CCI vary 5-50% depending on footprint method



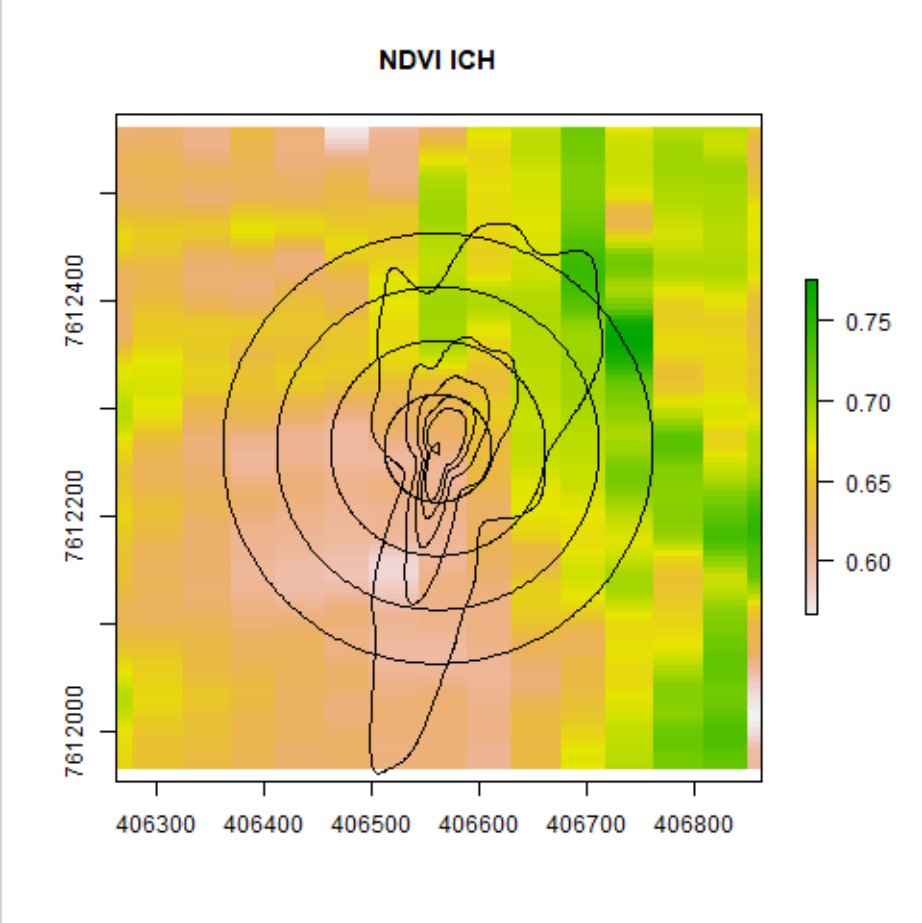
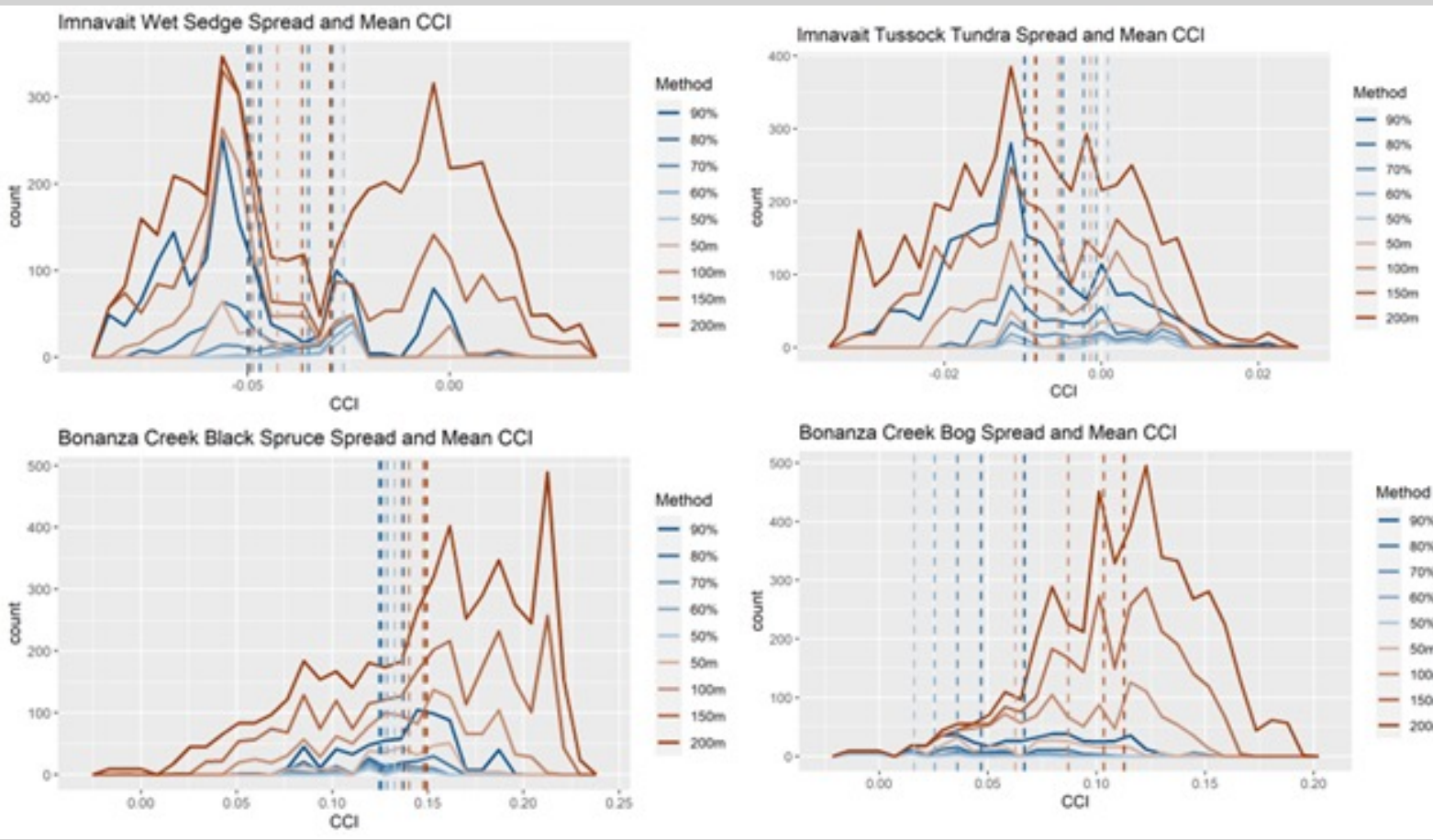
Atqasuk Percent Difference from 50% 7.8.17 NDVI



Atqasuk Percent Difference from 50% 7.8.17 CCI

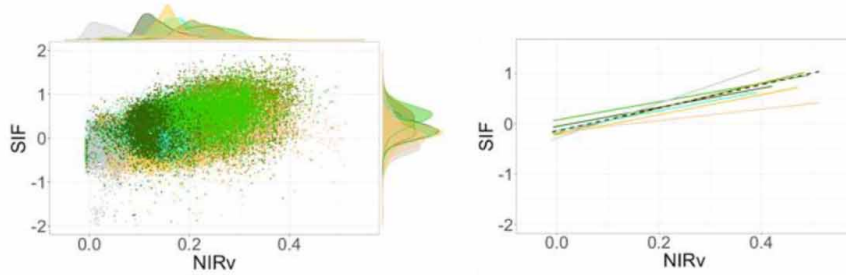


An example from 4 sites shows pixel counts using different footprints. Take home: How you compare flux tower data to remote sensing data matters. Recommend using weighted footprints.



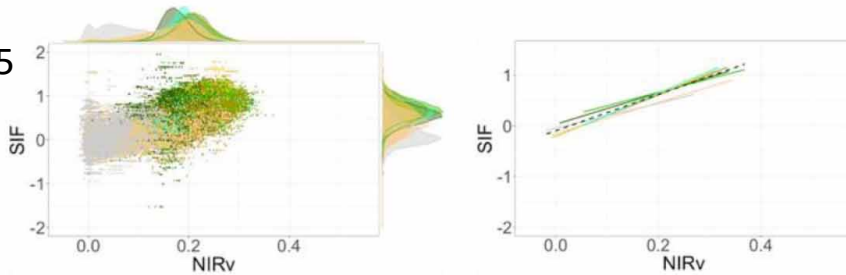
Y-axis = % contour or radii distance from tower

$R^2_{\text{air}}(\text{NIRv}) = 0.26$



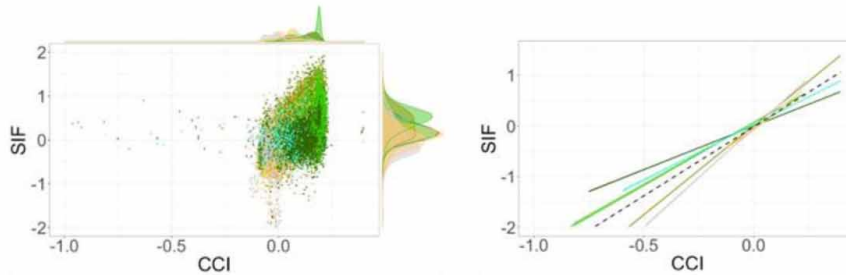
Landcover	R2	slope	% n
ALL	0.26	2.32	1.00
Evergreen Forest	0.13	1.91	0.29
Deciduous Forest	0.16	1.83	0.17
Shrubland	0.20	2.53	0.29
Herbaceous	0.08	1.12	0.05
Sparsely Vegetated	0.09	1.99	0.07
Barren	0.44	3.51	0.04
Fen	0.14	1.92	0.09

$R^2_{\text{space}}(\text{NIRv}) = 0.5$



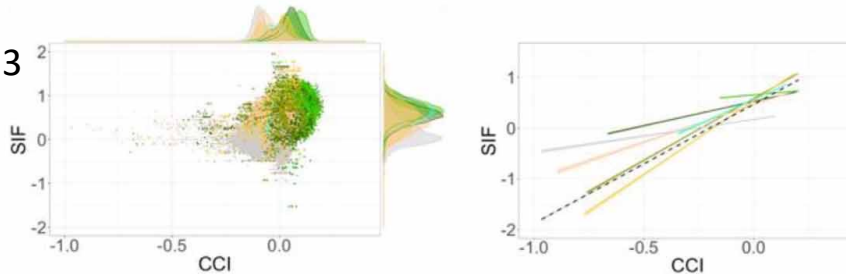
Landcover	R2	slope	% n
ALL	0.50	3.57	1.00
Evergreen Forest	0.18	3.09	0.35
Deciduous Forest	0.18	2.66	0.11
Shrubland	0.32	4.05	0.18
Herbaceous	0.39	3.07	0.09
Sparsely Vegetated	0.50	4.13	0.06
Barren	0.24	2.45	0.18
Fen	0.27	4.29	0.04

$R^2_{\text{air}}(\text{CCI}) = 0.18$



Landcover	R2	slope	% n
ALL	0.18	1.48	1.00
Evergreen Forest	0.09	1.08	0.29
Deciduous Forest	0.02	0.46	0.17
Shrubland	0.25	2.35	0.29
Herbaceous	0.39	3.54	0.05
Sparsely Vegetated	0.33	3.01	0.07
Barren	0.04	0.43	0.04
Fen	0.09	0.96	0.09

$R^2_{\text{space}}(\text{CCI}) = 0.3$



Landcover	R2	slope	% n
ALL	0.30	2.35	1.00
Evergreen Forest	0.04	0.95	0.35
Deciduous Forest	0.01	0.39	0.11
Shrubland	0.24	2.44	0.18
Herbaceous	0.09	1.48	0.09
Sparsely Vegetated	0.35	2.97	0.06
Barren	0.02	0.67	0.18
Fen	0.16	1.96	0.04

Spatial Covariation between Solar-induced Fluorescence and Vegetation Indices from Arctic-Boreal Landscapes

AJ Maguire, JUH Eitel, TS Magney, C Frankenberg, P Kohler, EL Orcutt, NC Parazoo, R Pavlick, and ZA Pierrat. 2021.

Environmental Research Letters

What is the scale dependance among remote sensing metrics commonly used to infer productivity?

- SIF (TROPOMI, CFIS), CCI and NIRv (AVIRIS, MODIS)

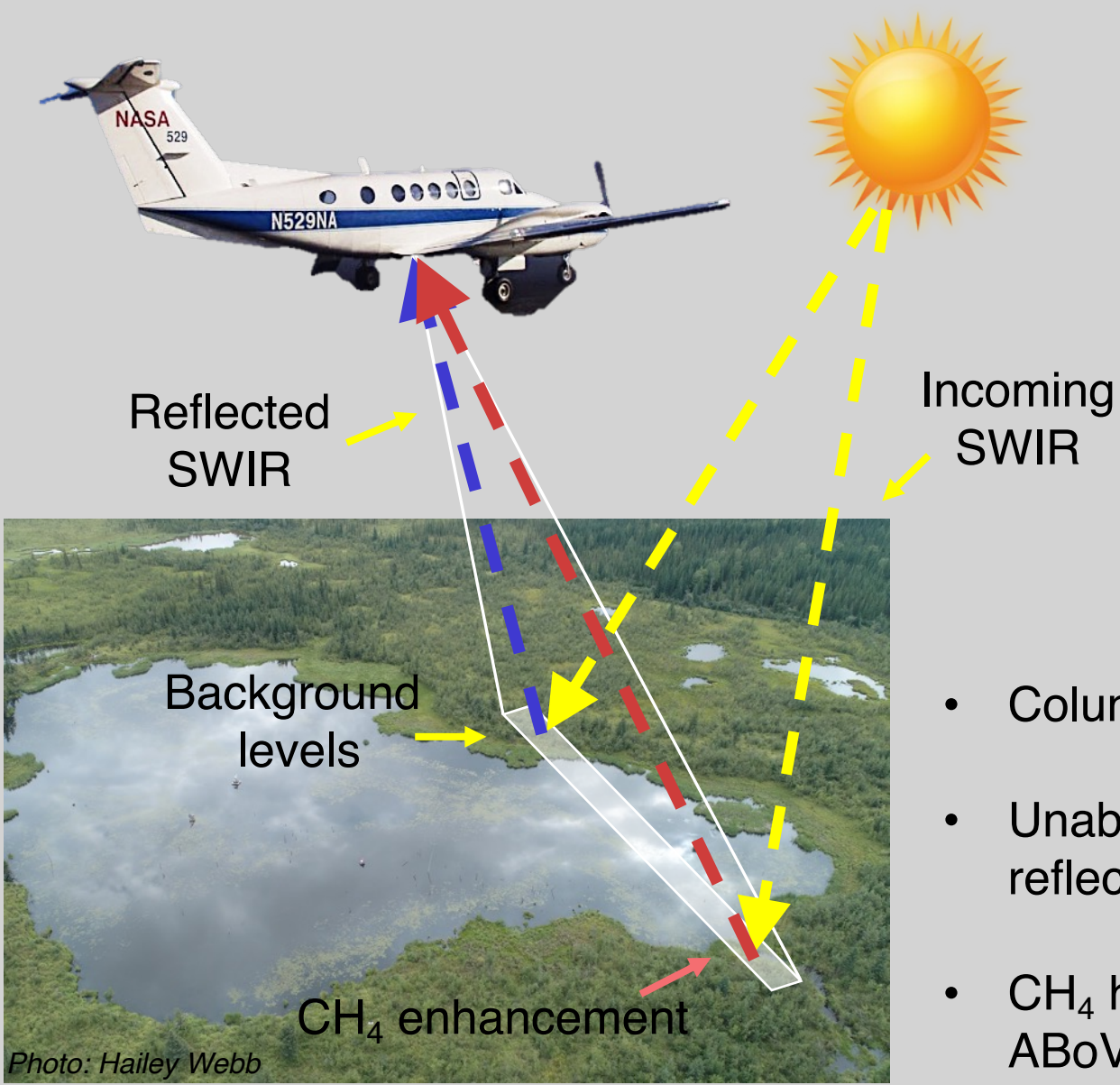
Finding: Linearity of SIF-CCI and SIF-NIRv relationship generally degrade as you move from satellite to airborne scale, with considerable variation among cover types.

Limitation of moderate resolution observations to capture spatial variance in photosynthetic activity.

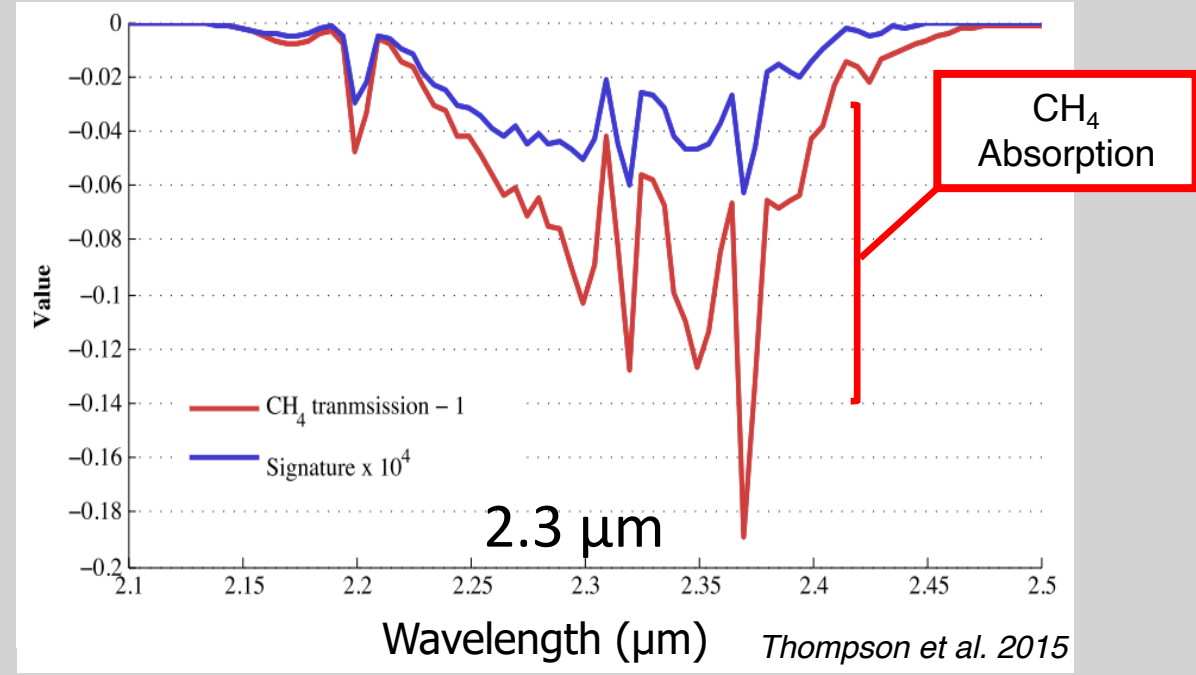


Methane Emissions

- Detection of CH₄ hot spots in permafrost landscapes (wetlands)
 - Related to geomorphology: talik and thermokarst undercutting features
- Chip Miller, Clayton Elder, Latha Baskaran, Andrew Thorpe, David Thompson + collaborators
- Elder et al. 2020, *Geophysical Research Letters*, <https://doi.org/10.1029/2019GL085707>
- Elder *et al.*, 2021, *Global Biogeochemical Cycles*, <https://doi.org/10.1029/2020GB006922>
- Baskaran et al., 2022, *Environmental Research Letters*, <https://doi.org/10.1088/1748-9326/ac41fb>



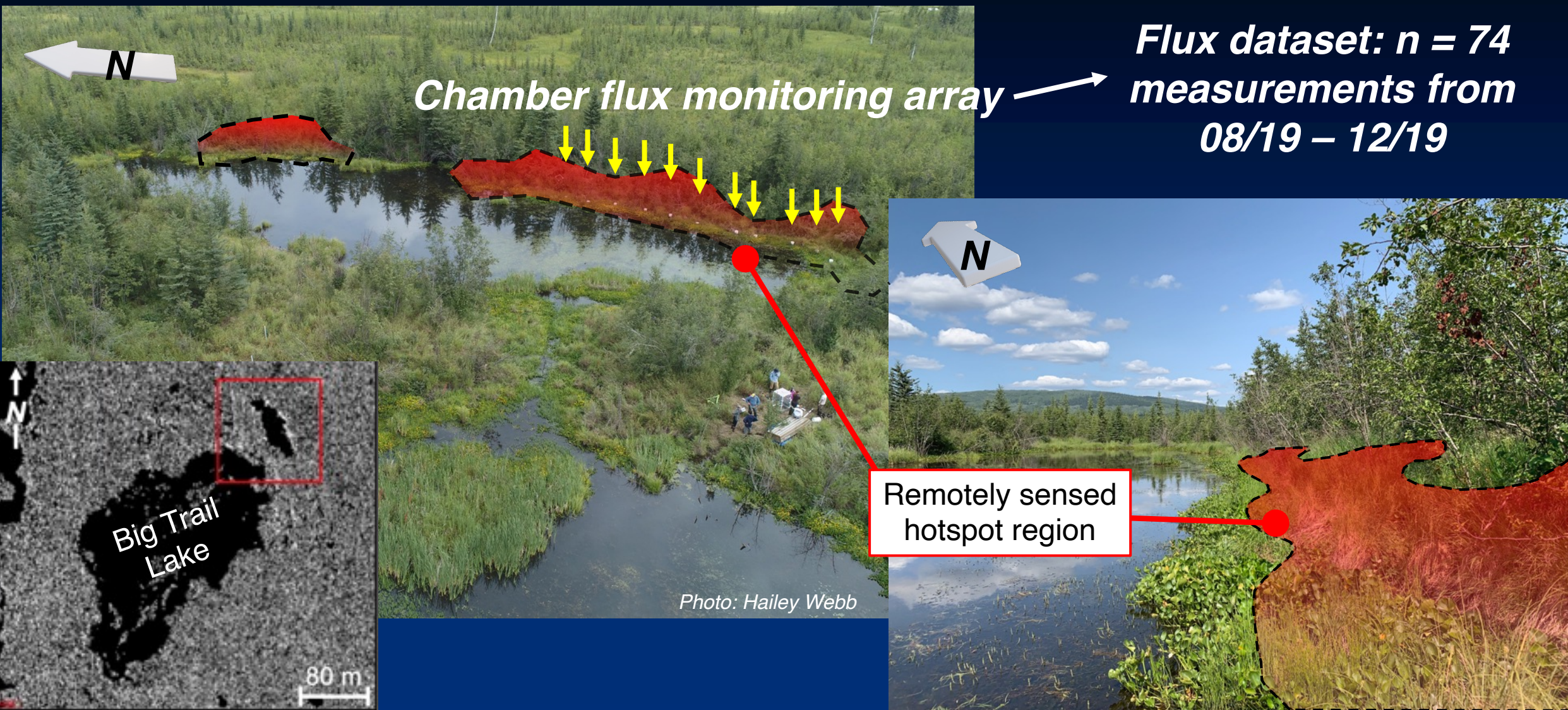
Column CH₄ Enhancement due SWIR absorption



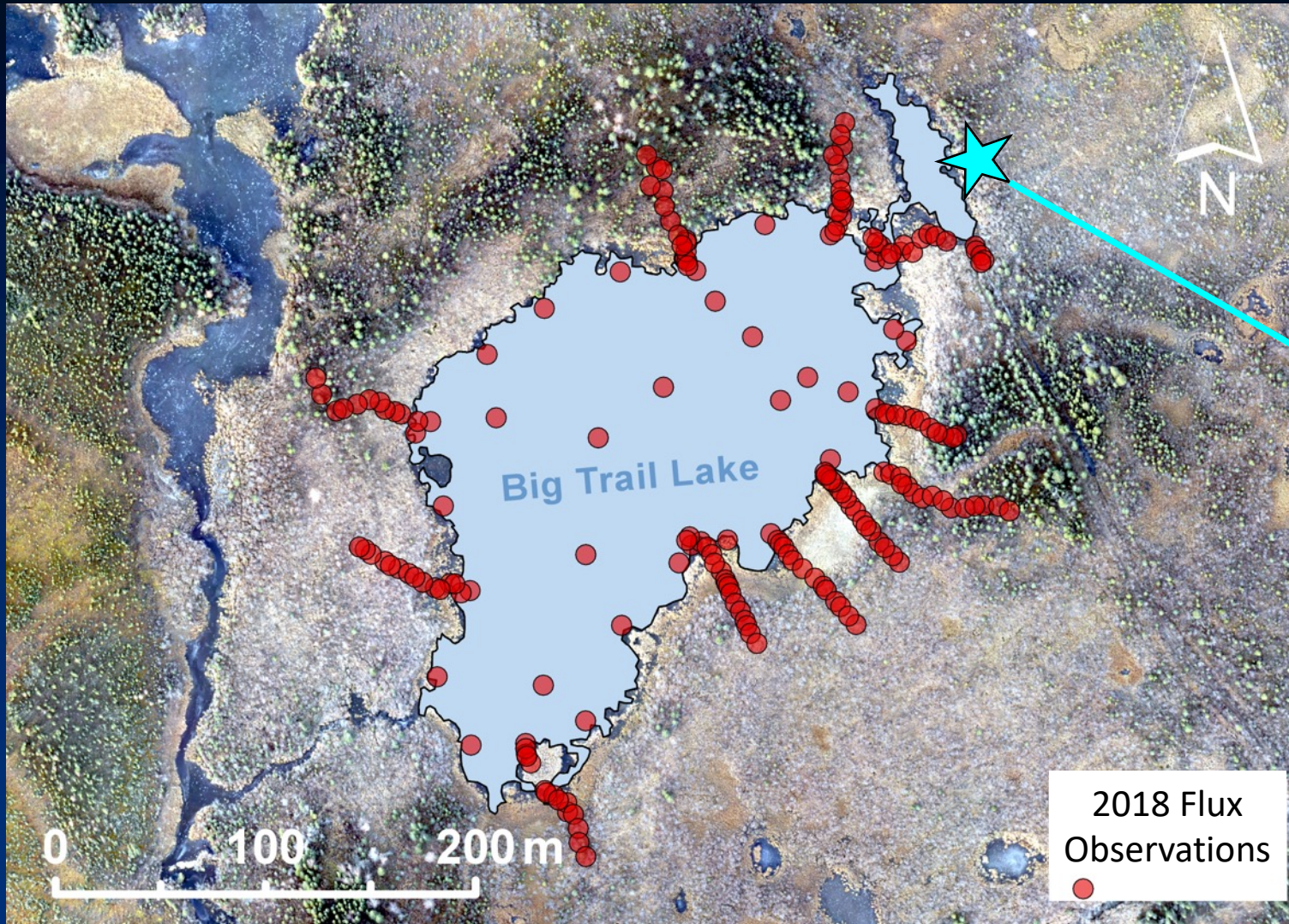
- Column-integrated path-length units of ppm m
- Unable to detect CH₄ over water surfaces (no SWIR reflection)
- CH₄ hotspot detection threshold 2000 – 3000 ppm m in the ABoVE domain



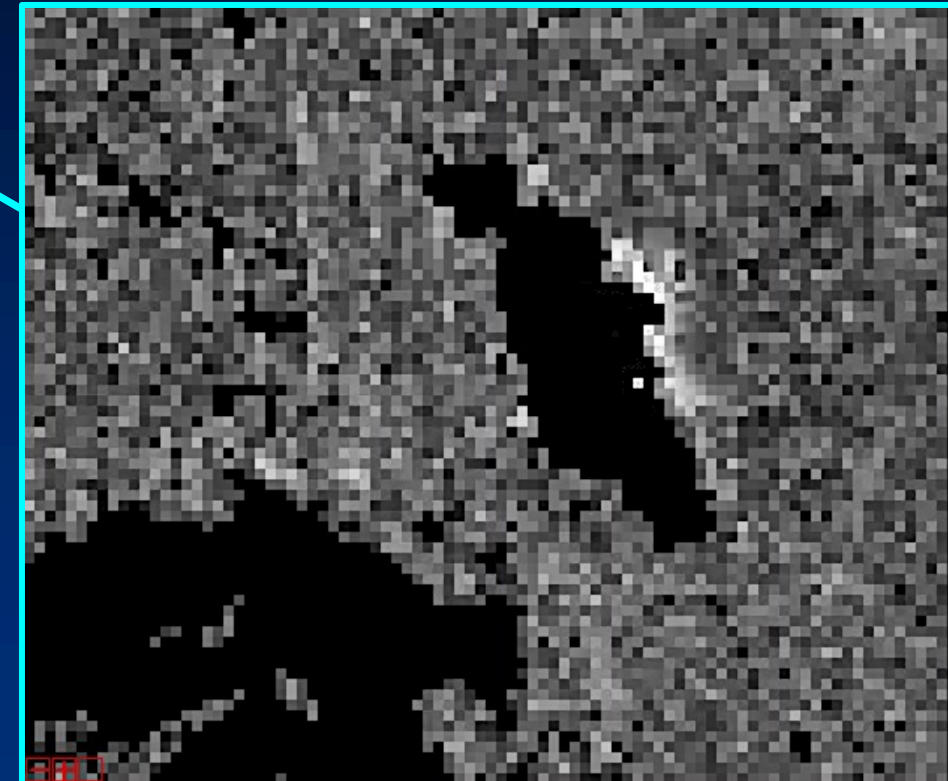
Overnight processing of initial 2019 AVIRIS-NG overflight data confirms persistent hotspot and motivates ground investigation



AVIRIS-NG detects CH₄ hotspot at field site in 2018



2018 AVIRIS-NG CH₄ Hotspot
at Big Trail Lake



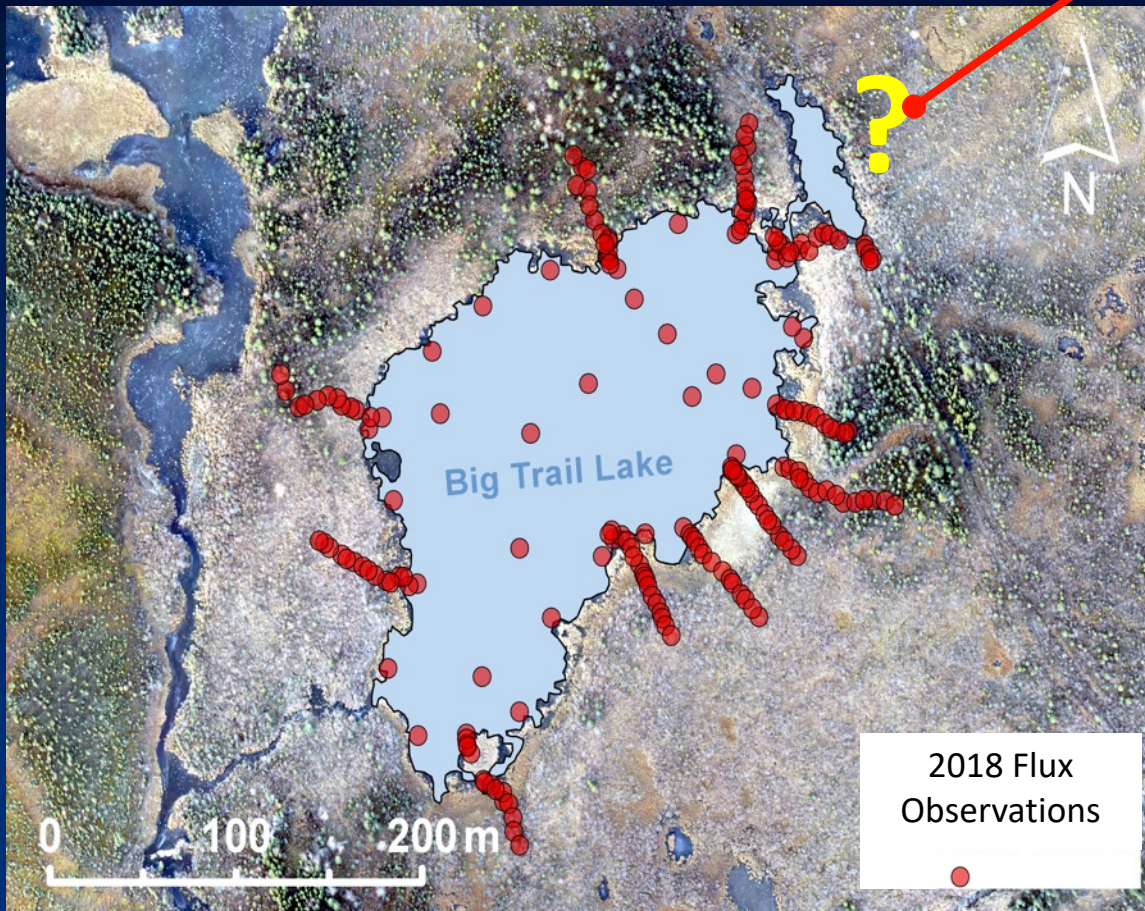
Bright pixels = enhanced CH₄



Ground validation of CH₄ hotspot patterns and fluxes at Big Trail Lake, AK

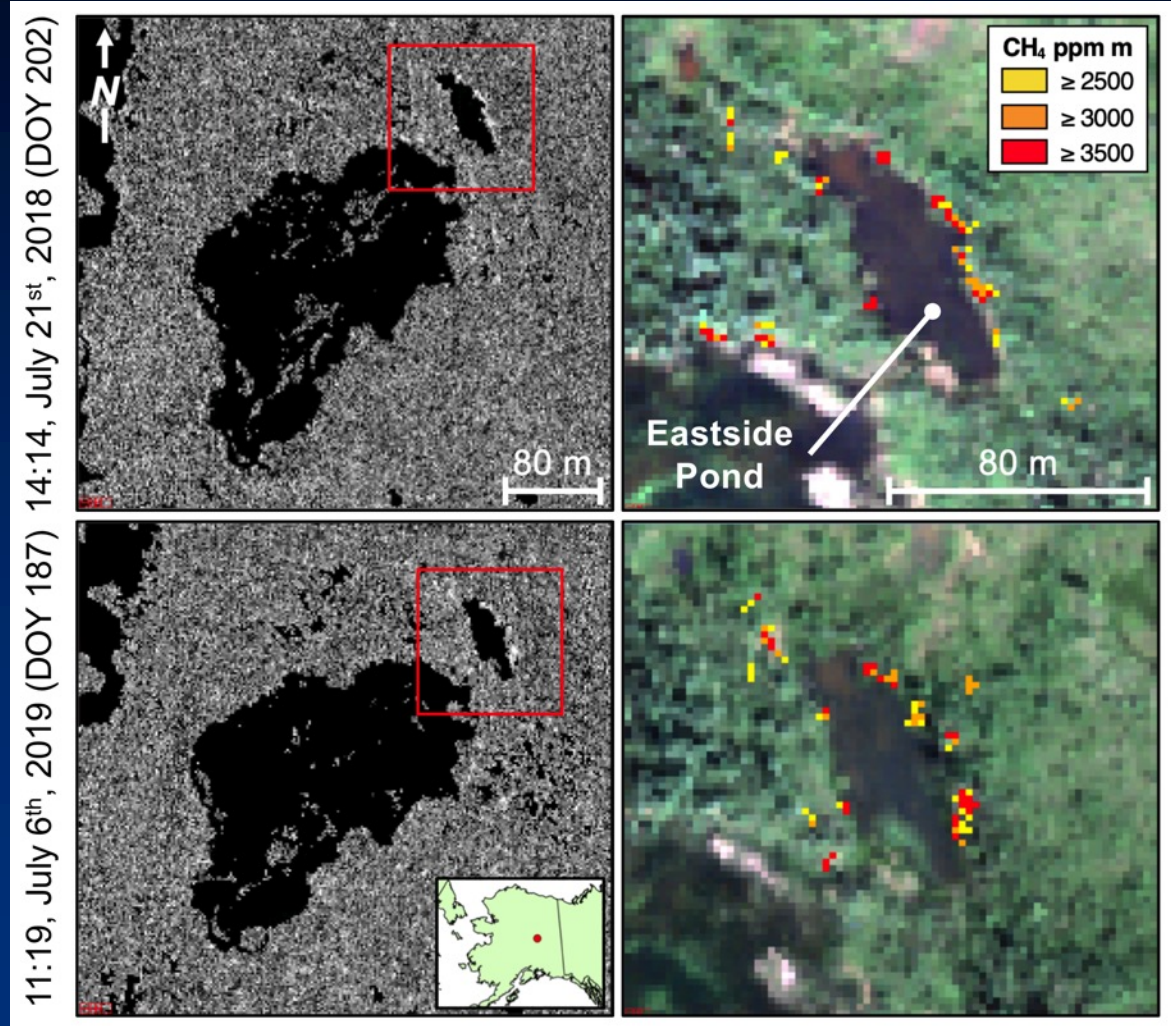
In-situ chamber flux monitoring initiated in 2018

without prior knowledge, 2018 ground survey misses hotspot



Elder et al. 2020

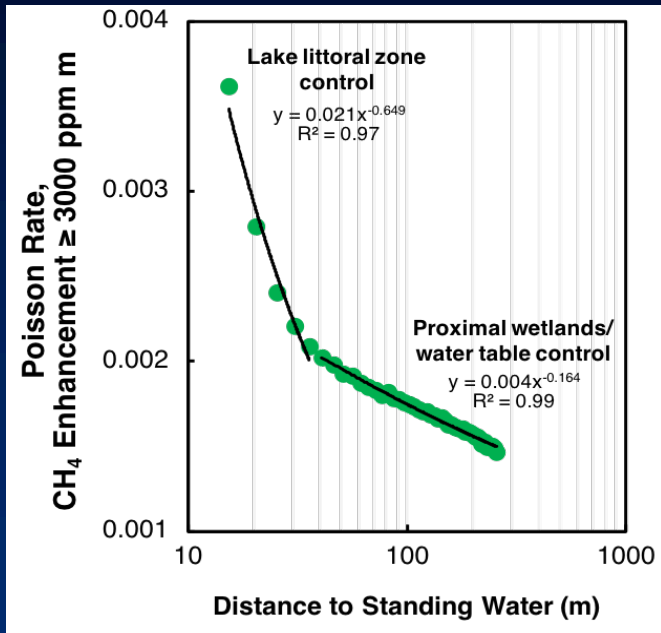
Persistent hotspot identified post 2018 field season and in subsequent 2019 surveys



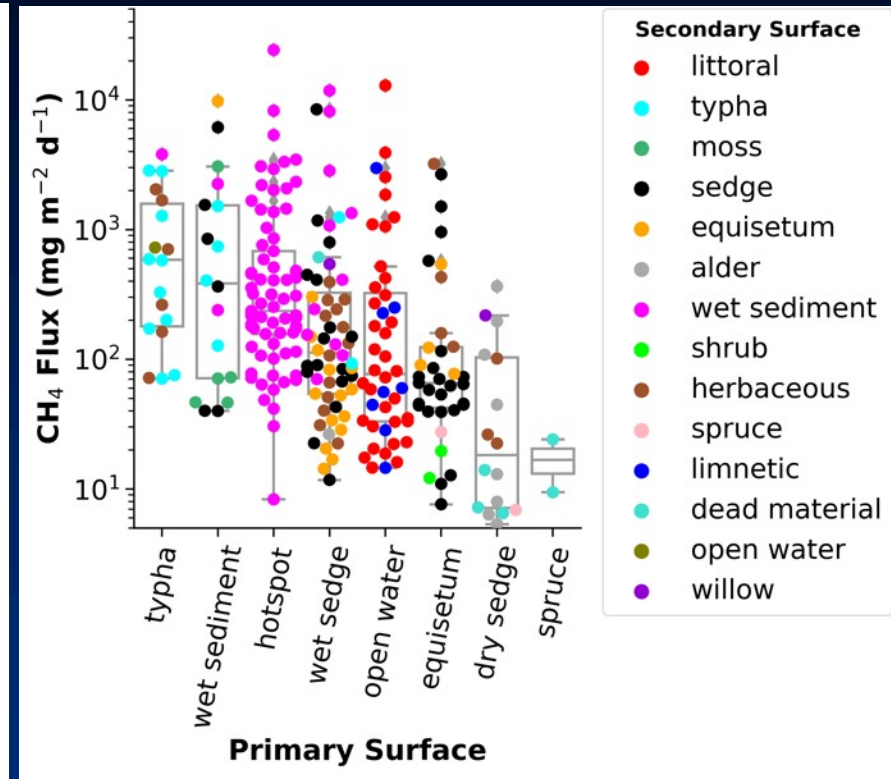
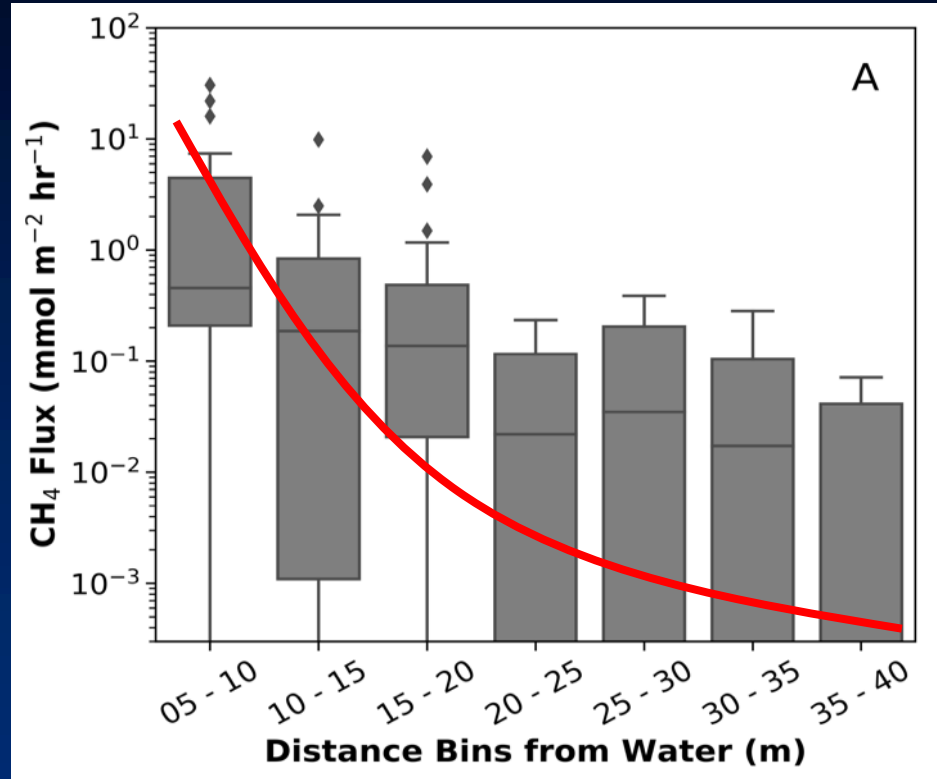
Elder et al. (In Review)

CH₄ Hotspots follow spatial power law with respect to distance from water, mirroring wide-ranging in situ fluxes

AVIRIS-NG Domain-wide Hotspot Pattern



In-Situ Flux Monitoring



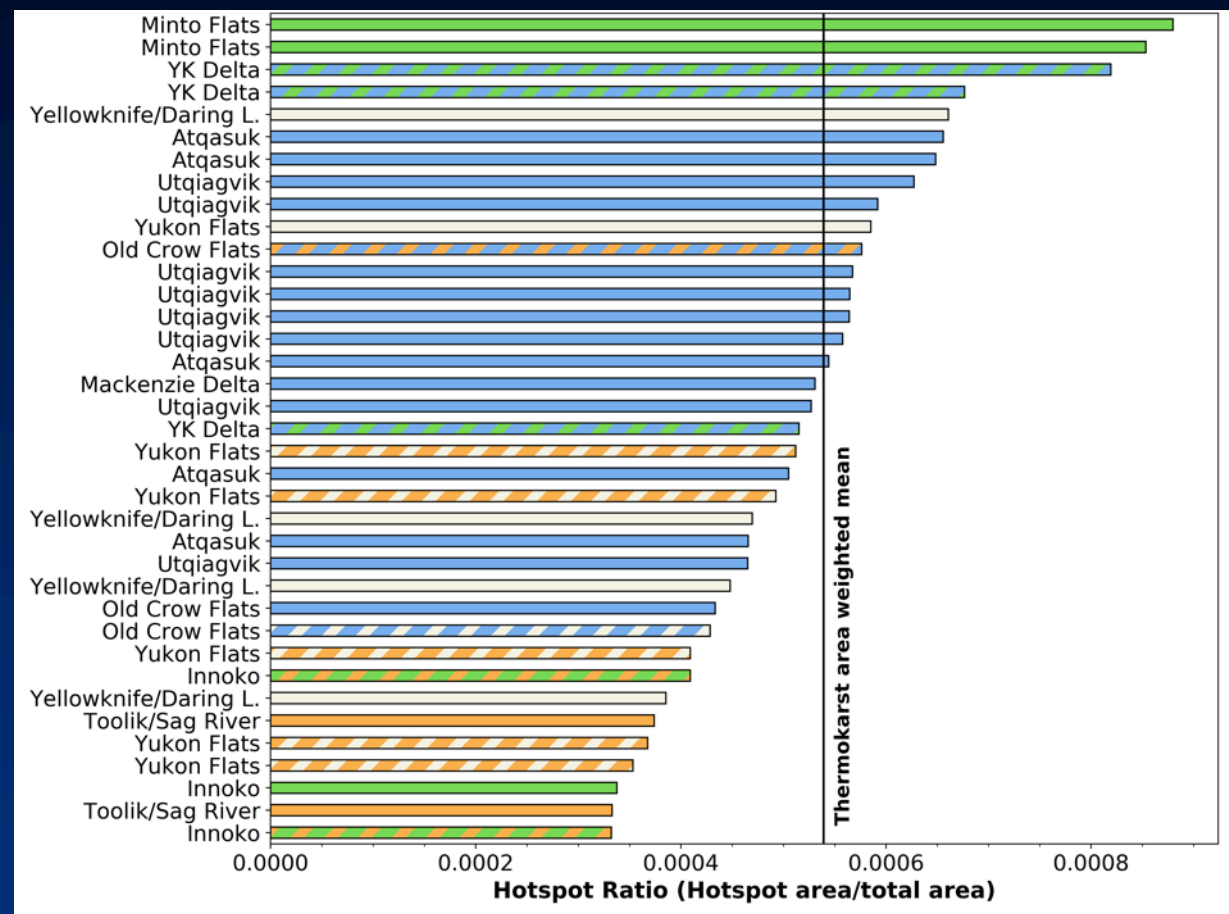
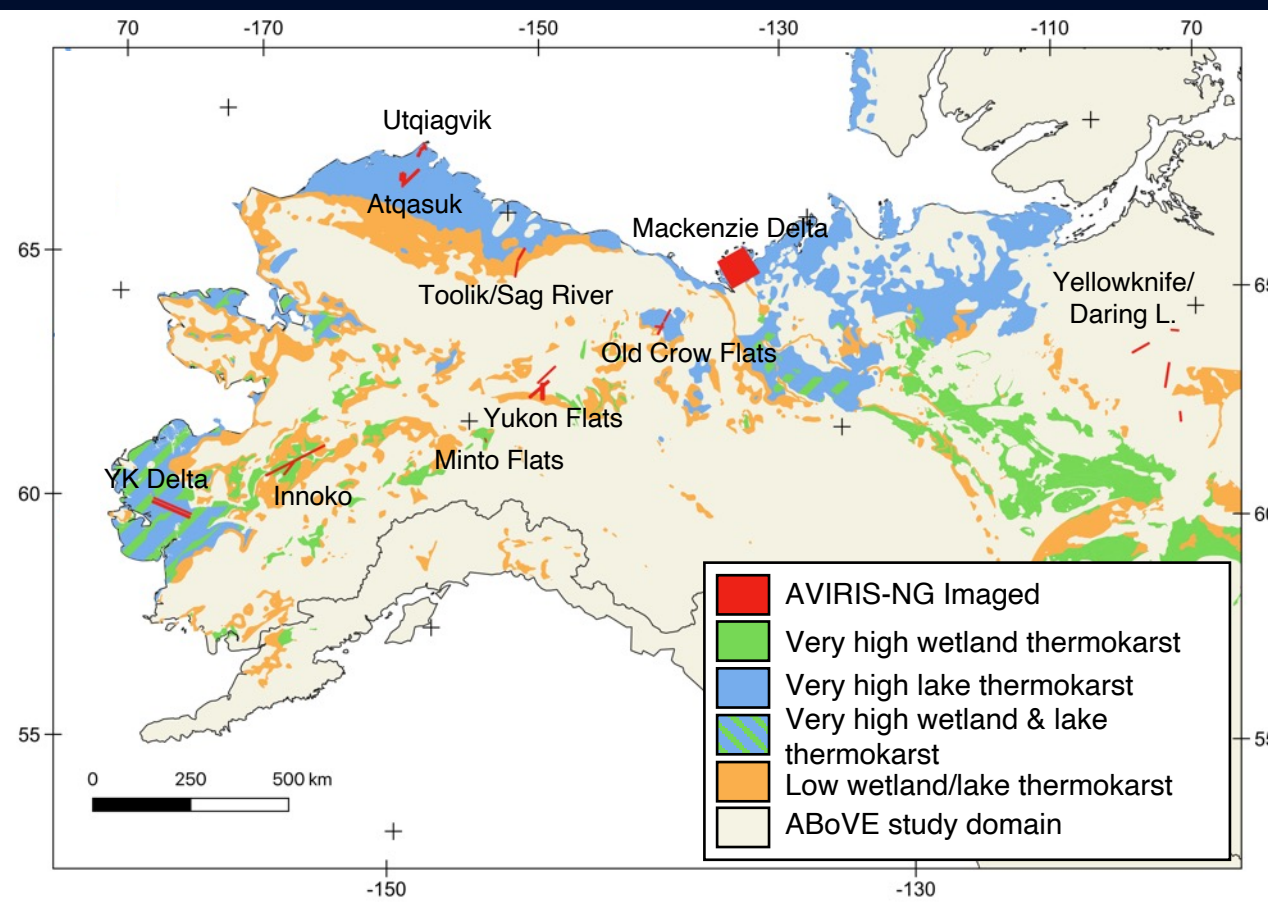
Remote power exponent

$$\alpha_{remote} = 0.65$$



Domain-wide AVIRIS-NG hotspot occurrence correlates with landscape-scale levels of thermokarst activity

Hotspot occurrence ratio was determined for a subset of 65 flight lines spanning variable levels of thermokarst.



Elder et al. (Submitted)

Hotspots were more prevalent in regions with very high wetland and lake thermokarst.

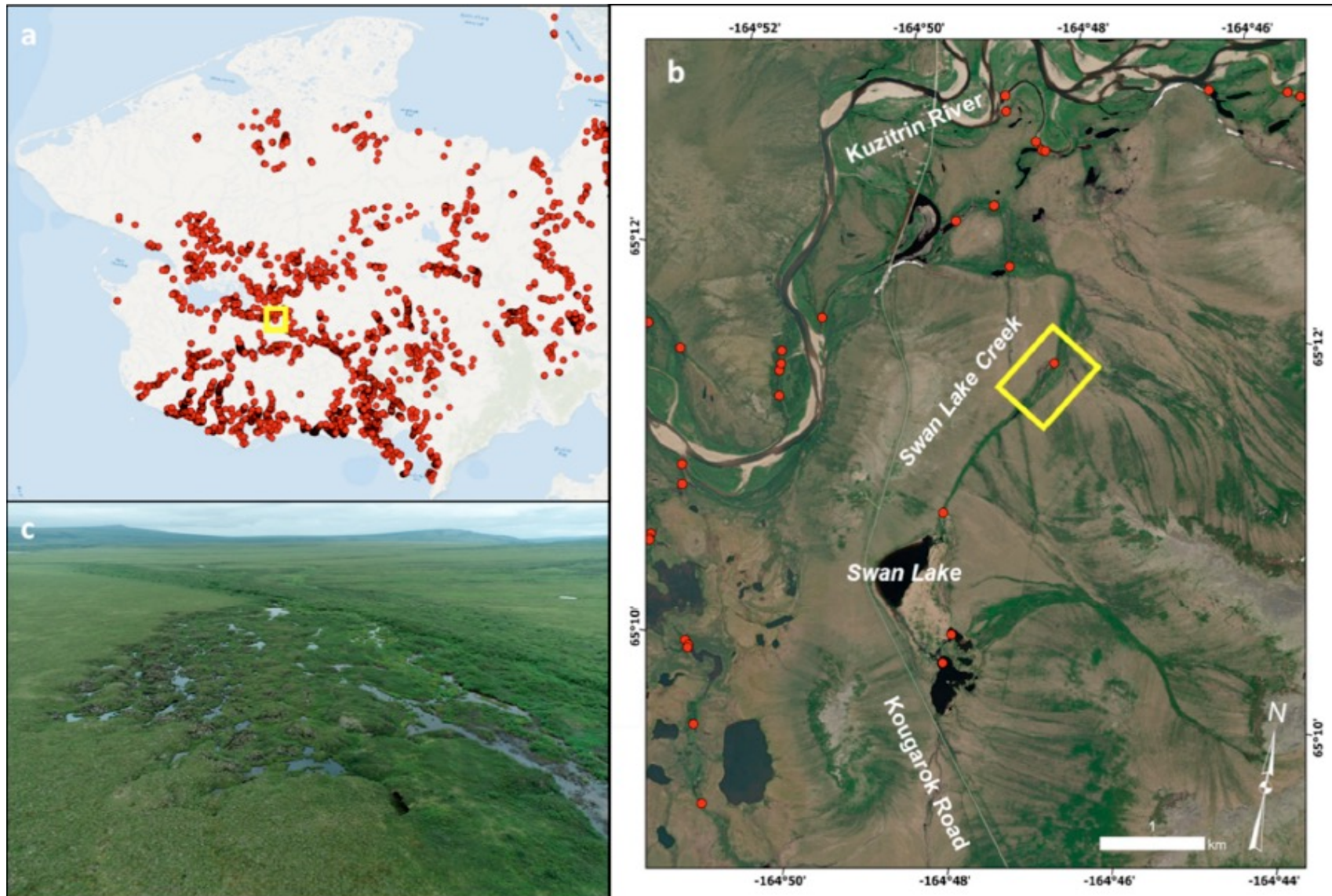


Using AVIRIS to study Beaver Engineering Disturbance and CH₄ Hotspots in NW Alaska



Similar tundra beaver disturbance – CH₄ hotspot studies are under way on the Seward Peninsula near Swan Lake and the NGEE-Arctic Kougarok site

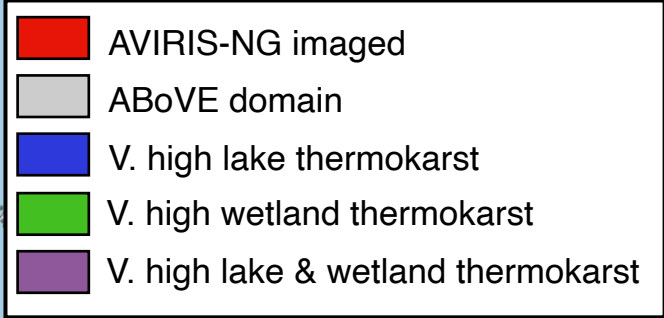
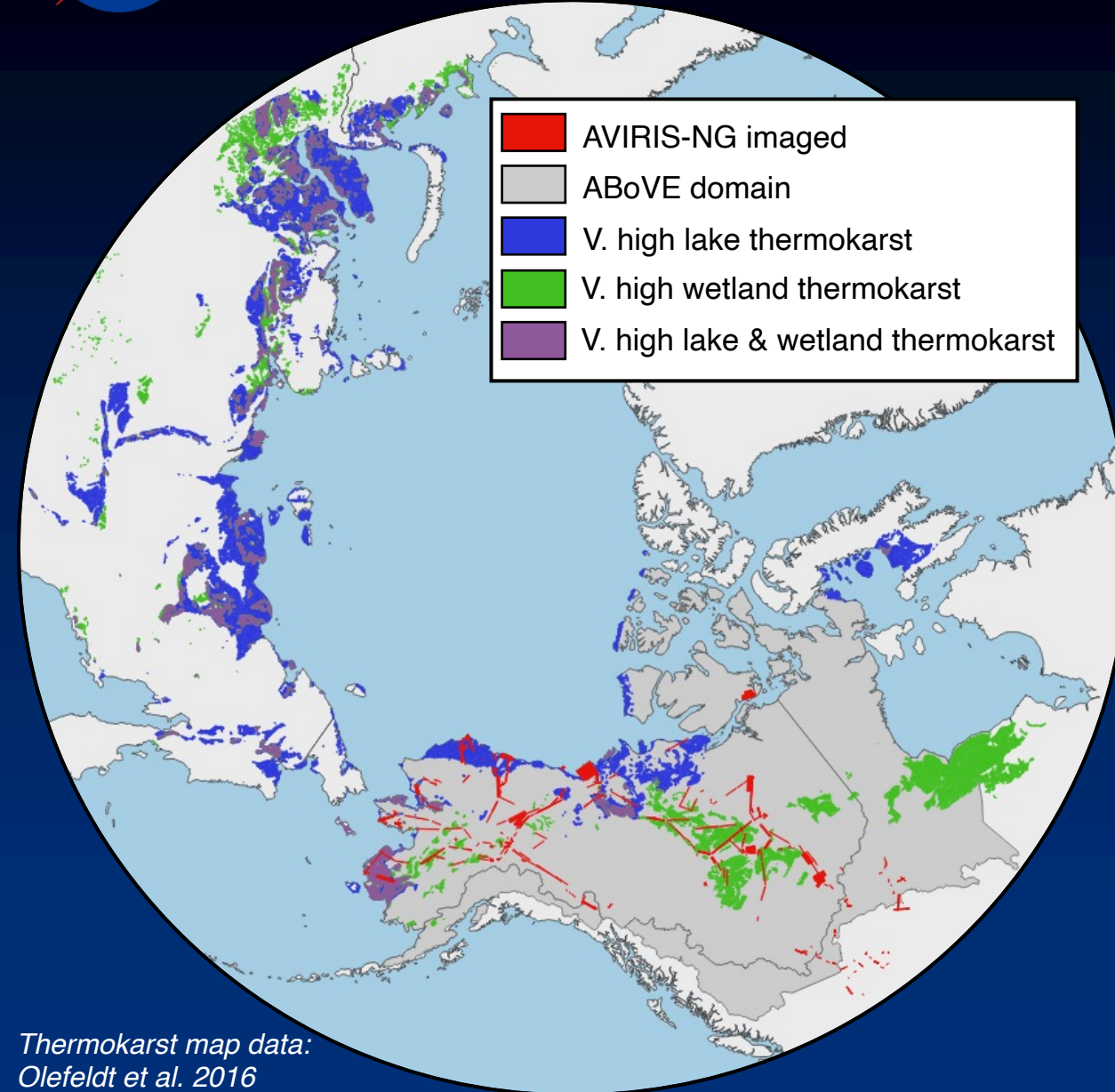
Correlating hydrologic changes with AVIRIS methane hotspots



Jones et al., Remote Sens (2021)



Upscaling CH₄ hotspot occurrence ratios across pan-Arctic regions of very high lake and/or wetland thermokarst



Upscaling Parameters

- Two upscaling area approaches: discrete features, areas highly susceptible to thermokarst
- Two hotspot occurrence ratios: discrete features, broad area
- Mean, mean of daily max, max in-situ observed flux rates
- 200 days of emissions (growing + cold season fluxes)

Upscaling area description	Upscaling area (m ²)	Hotspot occurrence ratio (%)	CH ₄ flux (mg m ⁻² d ⁻¹)	flux days ^{yr}	Pan-Arctic Hotspot Flux (g CH ₄ yr ⁻¹)	% of total wetland flux > 45° N*
Very high lake and/or wetland thermokarst occurrence	δ1.978 x10 ¹²	0.054 ^ψ	1168 ^a	200	2.5 x10 ¹¹	0.8
			7984 ^b		1.7 x10 ¹²	5.3
			24227 ^c		5.2 x10 ¹²	16.2
Active lake and wetland thaw features	β1.498 x10 ¹¹	0.243 ^φ	1168 ^a	200	8.5 x10 ¹⁰	0.3
			7984 ^b		5.8 x10 ¹¹	1.8
			24227 ^c		1.8 x10 ¹²	5.5
Median					1.14 x10 ¹²	3.6

pan-Arctic thermokarst hotspots emit roughly 1.0 Tg CH₄ yr⁻¹, or 4% of the pan-Arctic wetland CH₄ budget from < 0.005% of the northern permafrost region



ABOVE 9th SCIENCE TEAM MEETING

WYNDHAM SAN DIEGO BAYSIDE 23-26 JANUARY 2023

